Master of Science

Comparative Study of Stem Cell Conditioned Medium and Stromal Vascular Fraction in a Rat Model of Renal Ischemia-Reperfusion Injury

The Graduate School

of the University of Ulsan

Department of Medical Science

Yu Seon Kim

Comparative Study of Stem Cell Conditioned Medium and Stromal Vascular Fraction in a Rat Model of Renal Ischemia-Reperfusion Injury

Supervisor: Dalsan You

A Dissertation

Submitted to

the Graduate School of the University of Ulsan

In Partial Fulfillment of the Requirements

for the Degree of

Master of Science

by

Yu Seon Kim

Department of Medical Science

Ulsan, Korea

August 2022

Comparative Study of Stem Cell Conditioned Medium and Stromal Vascular Fraction in a Rat Model of Renal Ischemia-Reperfusion Injury

This certifies that the dissertation

of Yu Seon Kim is approved.

Jungyo Suh ·

Committee Chair M.D., M.S.

Nayoung Suh ·

Committee Member Ph D.

Dalsan You ·

Committee Member M.D., Ph D.

Department of Medical Science

Ulsan, Korea

August 2022

감사의 글

석사학위 논문이 완성되기까지 도움을 주신 많은 분들께 감사의 인사를 올립니다. 바쁘신 와중에도 귀한 시간을 내어 연구에 대해 따뜻한 격려와 조언을 주신 서준교 교수님, 서나영 교수님 그리고 많은 관심과 세심하고 힘있는 지도로 부족한 저를 따뜻하게 이끌어주신 유달산 교수님께 진심으로 감사 드립니다. 연구에 많은 도움과 지지를 주신 장명진 선생님, 김보현 선생님 모두 감사 드립니다.

ABSTRACT

Background: Conditioned medium (CM) therapy is emerging to avoid various adverse effects of cell-based therapies. Several studies have focused on using stem cell-derived CM in the treatment of various acute kidney injury (AKI) models. However, few studies compare the effects of cell-based and CM therapies in AKI. Therefore, we compared the effects of autologous stromal vascular fraction (SVF) and adipose-derived stem cell (ADSC)-derived CM prepared using the three-dimensional spheroid culture system on the renal function of rats with renal ischemia-reperfusion injury (IRI)-induced AKI.

Materials and Methods: Fifty male Sprague Dawley rats were randomly divided into five groups: sham, nephrectomy control, IRI control, SVF, and ADSC-CM. The SVF and ADSC were isolated and cultured using each rat's paratesticular fat. The ADSC-CM was prepared using the three-dimensional spheroid culture system. Vehicle (IRI control), SVF, and ADSC-CM were injected into renal parenchyme. The renal function of the rats was evaluated 28 days before and 1, 2, 3, 4, 7, and 14 days after the surgical procedure. The rats were sacrificed 14 days after the surgical procedure, and kidney tissues were collected for histological examination.

Results: The renal parenchymal injection of ADSC-CM significantly reduced the serum blood urea nitrogen (BUN) level compared with the IRI control group on days 1, 2, 3, and 4 after IRI. The level of serum BUN was significantly lower in the ADSC-CM group than

in the SVF group on days 1 and 4 after IRI. The renal parenchymal injection of ADSC-CM significantly reduced the serum creatinine level compared with the IRI control group on days 1, 2, 3, and 4 after IRI. The serum creatinine level was significantly lower in the ADSC-CM group than in the SVF group 4 days after IRI. The renal parenchymal injection of ADSC-CM significantly increased the level of creatinine clearance (CrCl) compared with the IRI control group one day after IRI. The level of CrCl was significantly higher in the ADSC-CM group than in the SVF group one day after IRI. In addition, collagen content was significantly lower in the SVF and ADSC-CM groups than in the IRI control group in the cortex and medulla. Apoptosis was significantly decreased, and proliferation was significantly increased in the SVF and ADSC-CM groups compared to the IRI control group in the cortex and medulla. The expressions of anti-oxidative makers such as glutathione reductase and glutathione peroxidase were higher in the SVF and ADSC-CM groups than in the IRI control group in the cortex and medulla.

Conclusions: The renal function was effectively rescued through the renal parenchymal injection of ADSC-CM by the enhanced anti-fibrotic, anti-apoptotic and anti-oxidative effects. The ADSC-CM was superior to SVF in terms of serum BUN, creatinine, and CrCl in early phases after renal IRI, but the differences disappeared after seven days from IRI.

CONTENTS

LIST OF FIGURES

INTRODUCTION

Acute kidney injury (AKI) is an abrupt loss of kidney function that develops within 7 days.[1] AKI incidence is approximately 5% to 20% in hospitalized patients and 20% to 50% in intensive care unit patients.[2,3] Renal ischemia-reperfusion injury (IRI) is a leading cause of perioperative AKI.[4] Renal IRI occurs in various clinical settings, such as major vascular, cardiac and hepatic surgeries, shock, sepsis, trauma, and kidney transplantation, because of an interruption of renal blood flow, followed by the subsequent reperfusion.[4] In urologic practices, renal ischemia with reperfusion is induced during kidney transplants, partial nephrectomy, and nephrolithotomy with early renal dysfunction. Current treatments are primarily supportive to reduce the damage of renal IRI during these surgeries. AKI treatments are comprised of a series of supportive measures without an insult-oriented therapy. However, timely reperfusion of the ischemic area at risk is still the major concern in clinical practices, strategies such as ischemic preconditioning and controlled reperfusion along with antioxidant, complement, or neutrophil therapies may significantly prevent or limit IRI damage in humans.[5]

Meta-analysis studies evaluating the therapeutic effect of mesenchymal stem cells (MSCs) in small animals with chronic or acute renal injury have shown the beneficial effect of MSC therapy on renal regeneration and functional recovery.[6] In preclinical studies treating AKI, MSC therapy has shown to be beneficial through acting as an anti-inflammatory, antiapoptotic, anti-oxidative stress, antifibrotic, immunomodulatory, and proangiogenice. MSC treatment benefits have also been observed in clinical trials.[7] There are some safety issues that need to be explored before MSC can be used in humans, including tumorigenicity,[8] microbiological contamination,[9] putative profibrogenic potential,[10] and heterogeneity and functional diversity.[11]

Recent studies have suggested that adipose tissue-derived stromal vascular fraction (SVF)

might be an attractive cell source for cell-based therapies on account of the real-time isolation without *in vitro* expansion to avoid the risks of MSC treatments.[12-16] We found that renal function is effectively protected from renal IRI damage through the renal parenchymal injection of SVF.[17] However, some issues limit the use of SVF in humans, including decreased cell viability during freezing and thawing, immune rejection when using allogeneic cells, and putative thrombogenic potential.[18]

Conditioned medium (CM) therapy using soluble factors is emerging to avoid the various adverse effects of cell-based therapies, including MSC and SVF.[19] Several preclinical studies have focused on using stem cell-derived CM in the treatment of various AKI models.[20-22] Other preclinical studies have compared the effects of CM and cell-based therapies in AKI but have reported contradictory results.[23-25] Therefore, we compared the effects of autologous SVF and adipose-derived stem cell (ADSC)-CM on the renal function in a rat model of renal IRI-induced AKI. We were interested in using the three-dimensional (3D) spheroid culture system to attain more growth factors and cytokines in the ADSC-CM. The ADSC in the 3D spheroid culture system secretes more angiogenic and anti-apoptotic factors compared to the conventional two-dimensional (2D) culture system.[26]

MATERIALS AND METHODS

Animal Care and Study Design

All aspects of animal care, treatment, and surgical procedures followed the eighth edition of the *Guide for the Care and Use of Laboratory Animals*, published in 2011.[27] All animal experiments were approved by the Institutional Animal Care and Use Committee of the Asan Medical Center (2020-12-037). Fifty 8-week-old male Sprague-Dawley rats were purchased from Orient Bio Inc. (Seongnam, Korea, http://www.orient.co.kr) and housed for 1 week for acclimatization. During experiments, rats were maintained under a 12-hour light/dark cycle, lights on at 8 a.m. and off at 8 p.m., at a temperature of 22°C ± 2 , and a humidity level of 50%–55%, with ad libitum access to food and water.

At 9 weeks old, the rats were randomly divided into five groups with ten animals per group: sham, nephrectomy control, IRI control, SVF, ADSC-CM. Rats in the ADSC-CM group underwent bilateral paratesticular fat excision via a scrotal incision to culture ADSC and acquire CM. At 13 weeks old, rats in the SVF group underwent bilateral paratesticular fat excision via a scrotal incision to isolate SVF. At the same time, surgical procedures were performed to induce renal IRI. Vehicle (IRI control), SVF, and ADSC-CM were injected into the renal parenchyme. The renal function of all the rats was evaluated 28 days before and 1, 2, 3, 4, 7, and 14 days after surgical procedures. The rats were sacrificed 14 days after surgical procedures, and kidney tissues were then collected for histological examination. The study design is outlined in Figure 1.

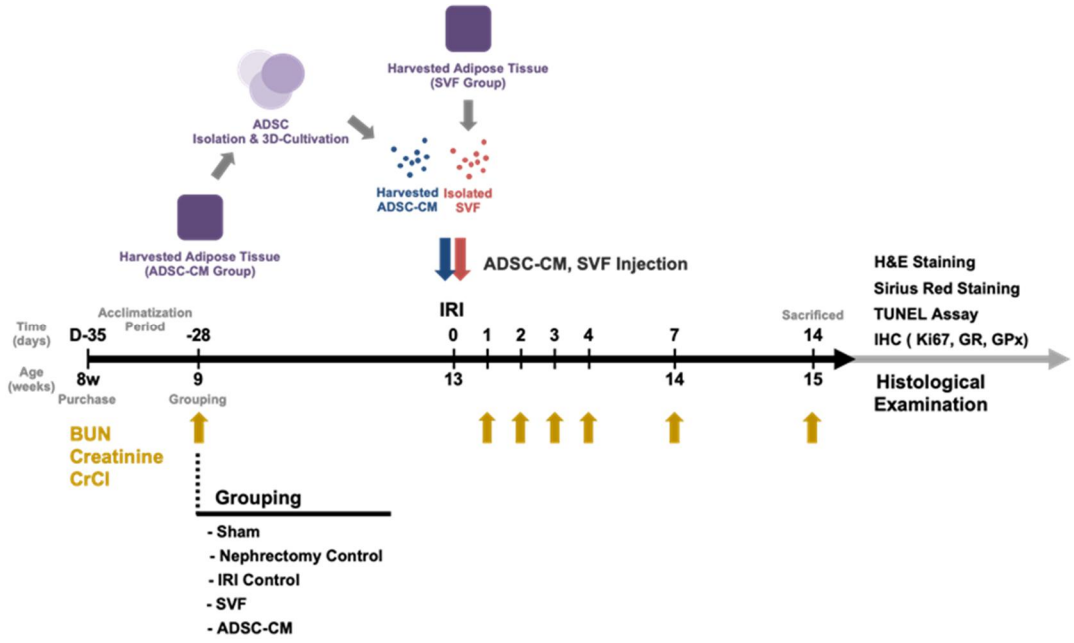

Figure 1. Graphic summary of the study design.

Abbreviations: ADSC, adipose-derived stem cell; 3D, three-dimensional; BUN, blood urea nitrogen; CrCl, creatinine clearance; IRI, ischemia-reperfusion injury; SVF, stromal vascular fraction; ADSC-CM, adipose-derived stem cell-conditioned medium; H&E, hematoxylin and eosin; TUNEL, terminal deoxynucleotidyl transferase dUTP nick end labeling; IHC, immunohistochemistry; GR, glutathione reductase; GPx, glutathione peroxidase.

Isolation of SVF and Cultivation of ADSC

Adipose tissue was harvested from paratesticular fats via a scrotal incision at randomization (ADSC-CM group) or shortly before the surgical procedure to induce renal IRI (SVF group). SVF was isolated, and ADSC was cultured as previously described.[28] Adipose tissue was enzymatically digested for 30 minutes at 37 in 0.075% collagenase type I (Thermo Fisher Scientific Inc., Waltham, MA, http://www.thermofisher.com). The cell suspension was passed through a 100 μm pore-sized filter to remove undigested tissue and then neutralized by the addition of Dulbecco's modified Eagle's medium (DMEM; Gibco, Waltham, MA, http://www.thermofisher.com) containing 10% fetal bovine serum (FBS; Gibco) and centrifuged at 3000 rpm for 10 minutes. The stromal cell pellet was resuspended in DMEM containing 10% FBS and 1% antibiotic-antimycotic solution (Gibco). Cultures were maintained at subconfluent levels (80%) at 37 in 5% CO . Cells were passaged using trypsin/EDTA (Thermo Fisher Scientific Inc.) as required. The resuspended cells were plated at a density of 2×10^3 cells per cm^2 and cultured in the conventional 2D culture system until passage number three.

Flow cytometry was performed with a FACScan argon laser cytometer (BD Biosciences, San Jose, CA, http://www.bdbiosciences.com) to determine whether the processed lipoaspirate cells were characteristic of SVF or ADSC according to a previous study.[29] Briefly, cells were harvested in 0.25% trypsin/EDTA and fixed for 30 minutes in ice-cold 2% formaldehyde. The fixed SVF was washed in flow cytometry buffer (2% bovine serum albumin, 0.1% sodium azide in phosphate-buffered saline (PBS)) and incubated for 30 minutes in flow cytometry buffer containing anti-CD45APC, CD34FITC, CD31PE-Cy7, and CD90PE (BD Biosciences). The fixed ADSCs were washed in flow cytometry buffer and incubated for 30 minutes in flow cytometry buffer containing anti-CD29Pacific Blue, CD44PE, CD45APC, and CD34FITC (BD Biosciences).

Differentiation of ADSC

Differentiation of ADSC was confirmed as described previously.[28] Briefly, ADSCs at the fourth passage were incubated with the StemPro Adipogenesis Differentiation Kit (Thermo Fisher Scientific Inc.) or StemPro Osteogenesis Differentiation Kit (Thermo Fisher Scientific Inc.) for 14 days, or the StemPro Chondrogenesis Differentiation kit (Thermo Fisher Scientific Inc.) for 21 days, and the media was changed every 3 to 4 days. Adipogenic differentiation was confirmed using Oil Red O (Sigma-Aldrich, St. Louis, MO, http://www.sigmaaldrich.com), osteogenic differentiation was confirmed using 2% alizarin red S (ScienCell, Carlsbad, CA, https://sciencellonline.com), and chondrogenic differentiation was confirmed using Alcian blue. The cells were photographed with an inverted microscope (Olympus, Tokyo, Japan, http://www.olympus-global.com).

3D Spheroid Culture and Preparation of CM

The ADSC-CM was prepared using ADSC spheroids as previously described.[30] A 12-series micro-mold (The 3D Petri Dish®; Merck KGaA, Darmstadt, Germany, https://www.merckgroup.com) was used to prepare microwells following the manufacturer's instructions. After the third passage, ADSCs were plated at 1×10^6 per well, and the microwells were incubated at 37 and 5% CO^2 for 3 days to induce cell spheroids. After aspirating the media, 2 mL of serum-free DMEM were added, and ADSC-CM was collected after 48 hours of incubation. The collected ADSC-CM samples were concentrated using 3 kDa cut-off centrifugal filter units (Merck KGaA) following the manufacturer's instructions. The Bradford assay reagent (Sigma Aldrich Co., St. Louis, MO, USA) was used to measure protein concentration in the CM. The ADSC-CM was stored at -80 until use.

Labeling and Tracking of SVF

SVF was labeled and tracked as previously described.[17] SVF was labeled with the fluorescent dye CM-DiI (Thermo Fisher Scientific Inc.). Cells were resuspended at a density of 1×10^6 cells per in serum-free DMEM. The cell suspension was then mixed with 5 μL of CM-DiI cell labeling solutions per mL and incubated at 37 for 30 minutes. An equal volume of serum-containing DMEM was added to stop the staining reaction. The labeled suspension was centrifuged, and the supernatant was removed. The cells were resuspended in serum-free DMEM and injected into the animals through each experimental route. Cross-sections of kidneys injected with CM-DiI-labeled SVF were observed using a fluorescent microscope.

Renal IRI Induction and Parenchymal Injection

Each rat was intramuscularly anesthetized with 0.3 mL of tiletamine (Zoletil; Virbac Laboratories, Carros, France, https://corporate.virbac.com) and xylazine hydrochloride (Rompun; Bayer, Leverkusen, Germany, https://www.bayer.com) in a 4:1 mixture. A laparotomy was performed in the sham group, and a right nephrectomy was performed in the nephrectomy control group. In the other three groups, a right nephrectomy was performed, and IRI of the left kidney was induced. IRI induction was performed in the left kidney as previously described.[16,17,31] For the renal parenchymal injection, a Hamilton syringe needle containing 100 μL of vehicle, SVF, or ADSC-CM was pierced from the lower pole to the upper pole of the kidney. While pulling out the needle, the contents were gradually released from the syringe.

Observation of Mortality and Measurements of Body Weight and Food Consumption

All rats were observed daily for mortality. Body weights were measured 28 days before and 1, 2, 3, 4, 7, and 14 days after surgical procedures. The food consumption was measured weekly before surgical procedures and during the observational period. The amount of food

consumed was estimated by subtracting the amount of leftover food from the amount of initially presented food.

Determination of Renal Function

Serum blood urea nitrogen (BUN) and serum and urine creatinine levels were measured 28 days before and 1, 2, 3, 4, 7, and 14 days after the surgical procedures. Urine was collected from the rats in a metabolic cage to estimate the 24-hour urine volume. The creatinine clearance (CrCl) was computed using the following formula and normalized to body weight:[32)]

CrCl (mL/min/100 g) = urine creatinine (mg/dL) × 24-hour urine volume (mL) × 100) / serum creatinine (mg/dL) × 1440 × body weight (g).

Kidney Harvest

The left kidney of all groups was harvested for histological examination. The weight of the left kidney was measured immediately after harvest. The kidney was cut in half, and the cross-section was visually observed. Half of each kidney was cryopreserved in liquid nitrogen, and the remaining half was fixed in 4% paraformaldehyde and embedded in paraffin. The renal index was computed using the following formula:[33)]

renal index (mg/g) = kidney weight (mg) / body weight measured 14 days after surgical procedures (g).

Hematoxylin and Eosin Staining and Histopathological Score

Kidney tissues were sectioned at 4 μm intervals, and hematoxylin & eosin staining was performed for microscopic analysis. After drying for 1 hour at 60℃, tissue sections were deparaffinized in xylene three times for 10 minutes each. After rehydrating with graded ethanol (100%, followed by 90% to 70%; 1 minute each), sections were washed three times

with distilled water. The sections were stained with Harris Hematoxylin solution (Sigma-Aldrich, St. Louis, MO) for five minutes, washed three times in distilled water, and then washed three times in a 0.5% acid alcohol solution followed by three washes in distilled water. After staining with Eosin Y solution (Sigma-Aldrich, St. Louis, MO) for ten seconds, the sections were rinsed with distilled water three times. The slides were dehydrated in ethanol solutions of increasing concentrations (70%, followed by 80%, 90%, and 100%). If there was insufficient staining, reverse staining was done. If the eosin stain was dense, sections were decolorized in absolute ethanol for 5 to 10 minutes. Finally, the sections were washed three times in xylene for 10 minutes. Sections were covered with a coverslip using Permount™ mounting medium. Histopathological scores were blindly estimated based on a previous study.[34] Histopathological scores were quantitated by calculating the degree of interstitial fibrosis, interstitial inflammation, tubular dilation, tubular basophilia, intratubular eosinophilic granules, and glomerulus degeneration in ten randomly chosen non-overlapping fields.

Sirius Red Staining

Sirius red staining was performed as previously described.[17] After drying for 1 hour in 60 , the slides were washed three times in xylene and rehydrated in ethanol solutions for 1 minute each, 100%, 90%, 80%, 70%, and washed three times in distilled water. Then the slides were stained with Harris hematoxylin solution (Sigma-Aldrich, St. Louis, MO) for 5 minutes. The slides were rinsed three times in distilled water, and the area around the tissue was marked with a PAP pen. The slides were stained with 60 μL of Pico Sirius Red reagent and incubated for 20 minutes. After washing the slides twice in an acid solution, they were washed three times in distilled water and then dehydrated through graded ethanol (70%, 80%, 90%, and 100%). The sections were cleared by xylene three times for 10 minutes each and mounted using permanent mounting media.

Whole kidney slides of each rat were digitized with a Panoramic SCAN digital slide scanner (3DHISTECH Ltd., Budapest, Hungary, https://www.3dhistech.com), and the histological images were subsequently analyzed by panoramic case viewer software (3DHISTECH Ltd.) at 20 times magnification. Four randomly selected kidney cortex and medulla fields from each rat were photographed using 3DHISTECH's CaseViewer. All images were analyzed using Adobe Photoshop to quantify signals. The results of Sirius red staining were presented as the percentage of collagen-positive areas in the total area of the cortex or medulla of each field.

TUNEL Assay

Terminal deoxynucleotidyl transferase (TdT) -mediated dUTP nick end labeling (TUNEL) for the detection of apoptotic cells was performed using an in situ cell death detection kit according to the manufacturer's protocol (Roche Molecular Biochemicals, Mannheim, Germany, https://life science.roche.com/shop/home). The TUNEL assay measured the degree of apoptosis in tissues due to renal IRI and was used to clarify the effect of SVF or ADSC-CM. Under light microscopy, TUNEL-stained sections were observed.

TUNEL staining was performed as previously described.[16] Unstained slides were placed in a 60 dryer and dissolved in paraffin for 1 hour to allow the tissue to adhere. Each sectioned specimen was deparaffinized in xylene for 10 minutes three times and rehydrated for 1 minute in ethanol solutions of decreasing concentrations (100%, 90%, 80%, and 70%). The sections were washed in distilled water for three minutes. For antigen retrieval, the slides were placed into the pretreatment solution, incubated for 5 minutes in a microwave oven and then cooled for 10 minutes. Next, the sections were washed in a wash buffer for 5 minutes. After washing, the protein blocking serum-free ready-to-use (Dako, Glostrup, Denmark, http://www.dako.com) reagent containing 20% FBS was added to the sections, and the sections were incubated in a humid chamber for 30 minutes. The sections were washed in

PBS for 5 minutes and gently wiped dry after removal from the buffer. Subsequently, 50 μL of the tunnel reaction mixture was added to the slides and incubated in a 37 humid chamber for 1 hour. The slides were rinsed in PBS for 5 minutes. Next, 50 μL of Converter-Peroxidase (Converter-POD) was added and incubated in a 37 humid chamber for 30 minutes. The slides were covered with parafilm (Bemis company inc., Oshkosh, WI, http://www.bemis.com) and washed with fresh PBS three times. Then, 50 μL of DAB working solution (substrate buffer 1 mL + DAB chromogen 20 μL) was added to the specimens and incubated for 10 minutes until the appropriate color appeared. The slides were washed three times in fresh PBS and counterstained with hematoxylin for 5 seconds. Afterward, the slides were washed three times in fresh PBS and dehydrated in ethanol solutions of increasing concentrations (70%, followed by 80%, 90%, 100%) for 1 minute each. Then the sections were cleared in xylene three times for 10 minutes and mounted using a prepared coverslip.

After staining, the slides were analyzed like the Sirius red staining. The results of the TUNEL assay were presented as the percentage of TUNEL-positive areas in the cortex or medulla of each field.

Immunohistochemistry

Immunohistochemistry staining was performed as previously described.[31] Kidney sections (4 μm thick) were prepared for immunohistochemistry analyses from rats of each group. Tissue sections were placed on microslides and deparaffinized in xylene, hydrated in serial decreasing concentrations of ethanol, and immersed in 3% H_2O_2 to quench endogenous peroxidase activity. Antigen retrieval was performed on all sections, and the slides were microwaved for 15 minutes in Tris-EDTA buffer (pH 9.0). Next, the sections were incubated for 2 hours at ambient temperature with anti-Ki67 (1:200, Abcam, Cambridge, MA, http://www.abcam.com), anti-glutathione reductase (GR; 1:2000, Abcam), or anti-

glutathione peroxidase (GPx; 1:2000, Abcam) antibodies. After washing, the slides were incubated using biotin-free polymeric horseradish peroxidase-linker antibody conjugate system (Dako) for 30 minutes at ambient temperature. The slides were washed, and chromogen development was performed for 10 minutes. The slides were counterstained with Meyer's hematoxylin and mounted using Immu-mount (Thermo Fisher Scientific Inc.).

After staining, the slides were analyzed like the Sirius red staining. The immunohistochemistry results were presented as the percentage of antibody-positive areas in the cortex or medulla of each field.

Statistical Analysis

Categorical variables are expressed as frequencies and percentages, and continuous variables as mean ± standard error. We used a one-way analysis of variance followed by Tukey's honest significant difference test for post hoc comparisons of multiple groups analyses. Statistical significance was defined as p less than 0.05, p less than 0.01, or p less than 0.001; p greater than or equal to 0.05 was not considered significant. All statistical analyses were performed using SPSS Statistics, version 21 (IBM Corporation, Armonk, NY, http://www-01ibm.com).

RESULTS

Characterization of SVF and ADSC

To characterize SVF and ADSC, CD marker profiles of SVF and ADSC were examined using flow cytometry. Flow cytometric analysis showed that SVF was made up of about half CD45+ cells (blood-derived cells), 23% CD45-/CD34+ (stromal cells), and 24.1% CD31+/CD34+ (endothelial cells). ADSC flow cytometric analysis showed that 99.2% of the cells expressed CD29, 63.9% expressed CD44, 1.7% expressed CD45, and 3.1% expressed CD34. The multilineage differentiation capacity was confirmed by observation of adipogenic, osteogenic, and chondrogenic cells 3 weeks after culture in the appropriate induction mediums (Figure 2).

A.

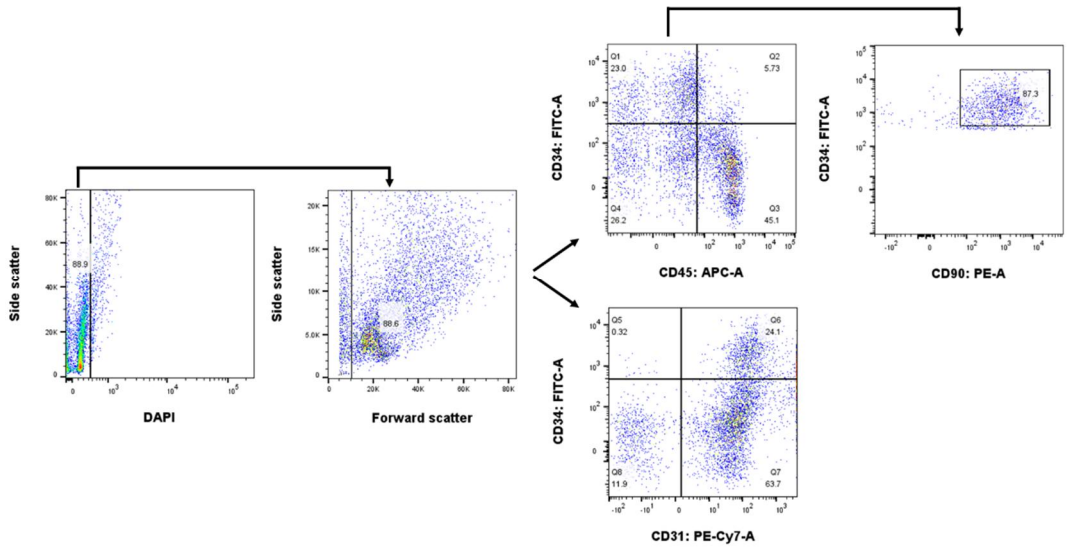
Side scatter
DAPI
Side scatter
Forward scatter
CD34: FITC-A
CD45: APC-A
CD34: FITC-A
CD90: PE-A
CD34: FITC-A
CD31: PE-Cy7-A

B.

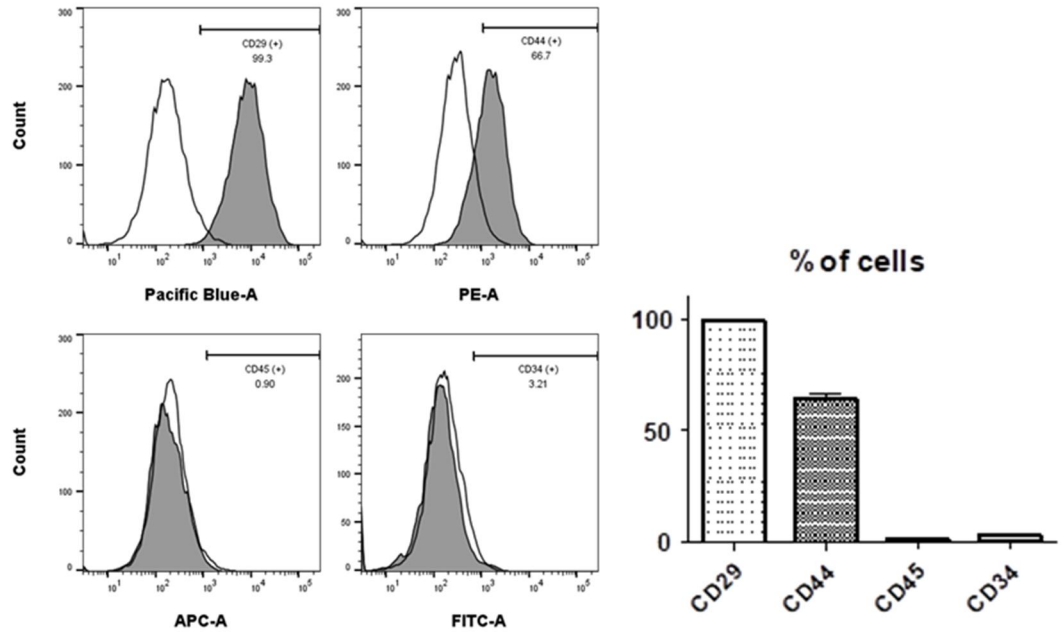
Count
CD29 (+)
99.3
Pacific Blue-A
CD44 (+)
66.7
PE-A
Count
CD45 (+)
0.90
APC-A
CD34 (+)
3.21
FITC-A
% of cells
100
50
0
CD29
CD44
CD45
CD34

C.

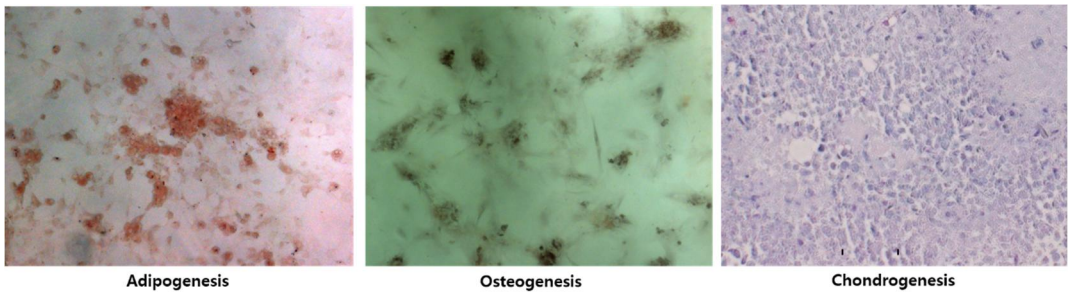

Figure 2. Characterization of SVF and ADSC. (A) Representative flow cytometry histograms of SVF from rats in the SVF group. (n=3) (B) Flow cytometry of ADSC from rats in the ADSC-CM group. Results are expressed as mean ± standard error. (n=9) (C) Appearance of ADSC from rats in the ADSC-CM group after three weeks of induction of adipogenic, osteogenic, or chondrogenic differentiation. Magnification, ×100 in adipogenesis and osteogenesis and ×400 in chondrogenesis. (n=3)

Abbreviations: ADSC, adipose-derived stem cell; SVF, stromal vascular fraction; ADSC-CM, adipose-derived stem cell-conditioned medium.

Mortality, Body Weight, and Food Consumption

One case in the ADSC-CM group experienced intraoperative death due to anesthesia (Figure 3A). The groups had no significant differences in body weight and food consumption (Figure 3B and C).

A.

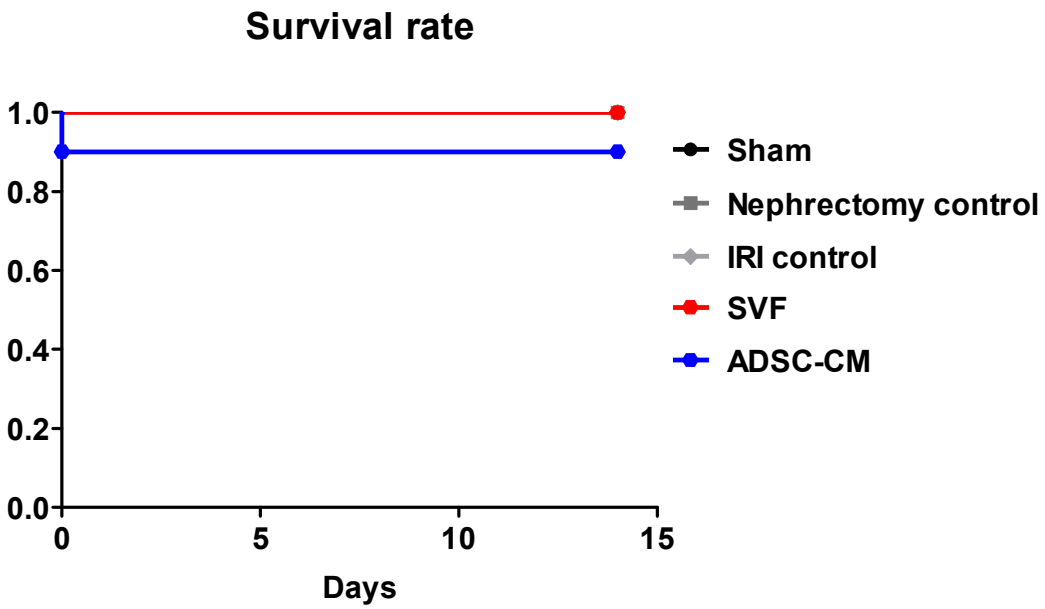
Survival rate
1.0
0.8
0.6
0.4
0.2
0.0
0
5
10
15
Days
Sham
Nephrectomy control
IRI control
SVF
ADSC-CM

B.

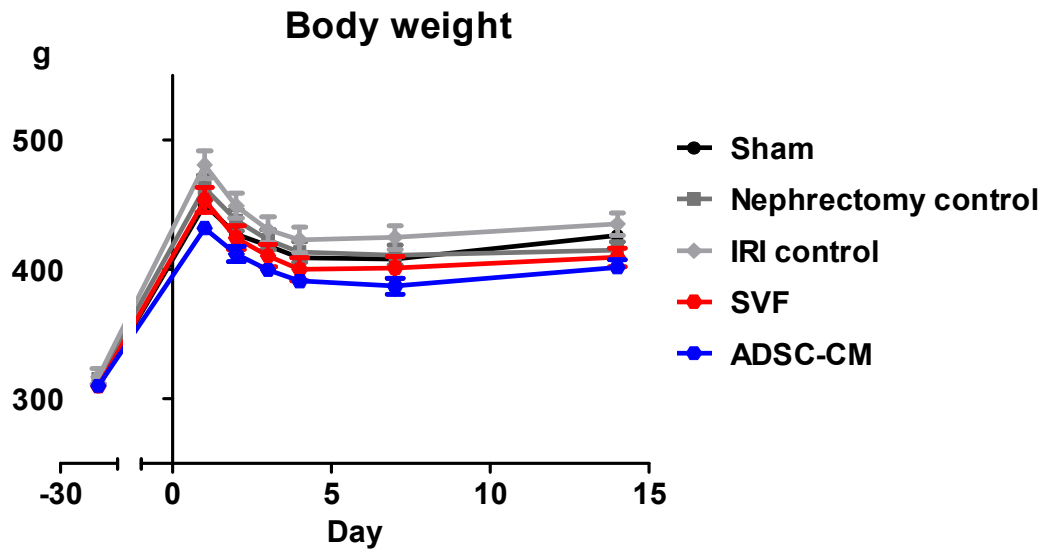
Body weight
g
500
400
300
-30
0
5
10
15
Day
Sham
Nephrectomy control
IRI control
SVF
ADSC-CM

C.

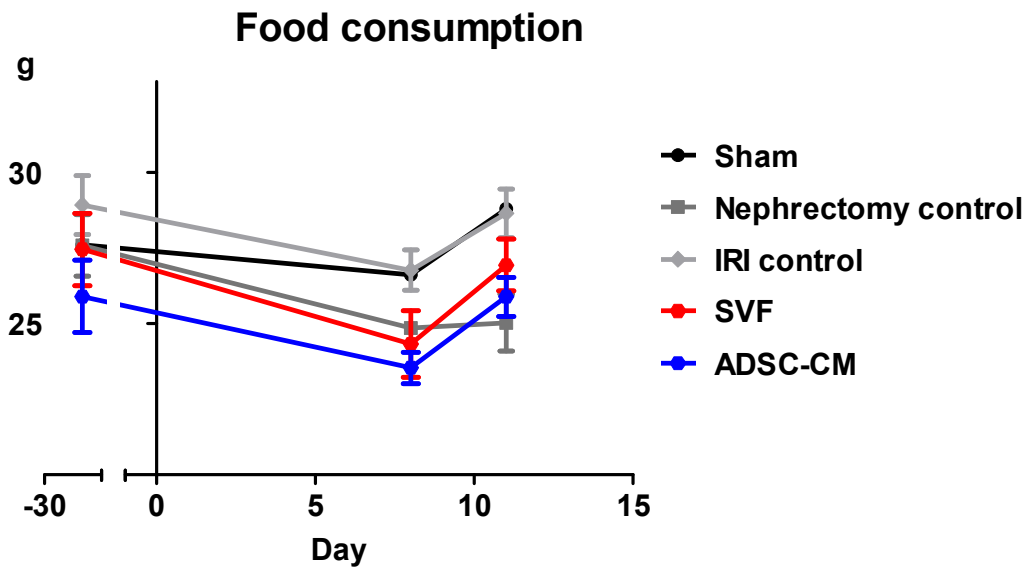

Figure 3. (A) Survival curves. (B) Changes in body weight, and (C) food consumption of each group during the experiment. Ten rats per group, but nine rats in the ADSC-CM group. Abbreviations: IRI, ischemia-reperfusion injury; SVF, stromal vascular fraction; ADSC-CM, adipose-derived stem cell-conditioned medium.

Effects of SVF and ADSC-CM on Renal Function

The renal parenchymal injection of ADSC-CM significantly reduced the levels of serum BUN compared with the IRI control group on days 1, 2, 3, and 4 after IRI (30.17 mg/dL vs. 53.96 mg/dL, $p < 0.001$; 25.77 mg/dL vs. 49.43 mg/dL, $p < 0.001$; 25.53 mg/dL vs. 38.44 mg/dL, $p < 0.001$; 22.03 mg/dL vs. 28.53 mg/dL, $p < 0.01$). The level of serum BUN was significantly lower in the ADSC-CM group than in the SVF group on days 1 and 4 after IRI (30.17 mg/dL vs. 47.34 mg/dL, $p < 0.01$; 22.03 mg/dL vs. 29.62 mg/dL, $p < 0.001$) (Figure 4A). The renal parenchymal injection of ADSC-CM significantly reduced the levels of serum creatinine compared with the IRI control group on days 1, 2, 3, and 4 after IRI (0.85 mg/dL vs. 1.24 mg/dL, $p < 0.001$; 0.78 mg/dL vs. 1.05 mg/dL, $p < 0.001$; 0.77 mg/dL vs. 0.91 mg/dL, $p < 0.001$; 0.70 mg/dL vs. 0.82 mg/dL, $p < 0.001$). Levels of serum creatinine were significantly lower in the ADSC-CM group than in the SVF group 4 days after IRI (0.70 mg/dL vs. 0.79 mg/dL, $p < 0.01$) (Figure 4B). The renal parenchymal injection of ADSC-CM significantly increased the level of CrCl compared with the IRI control group 1 day after IRI (0.22 mL/min/100 g vs. 0.16 mL/min/100 g, $p < 0.01$). The levels of CrCl was significantly higher in the ADSC-CM group than in the SVF group 1 day after IRI (0.22 mL/min/100 g vs. 0.17 mL/min/100 g, $p < 0.05$) (Figure 4C).

A.

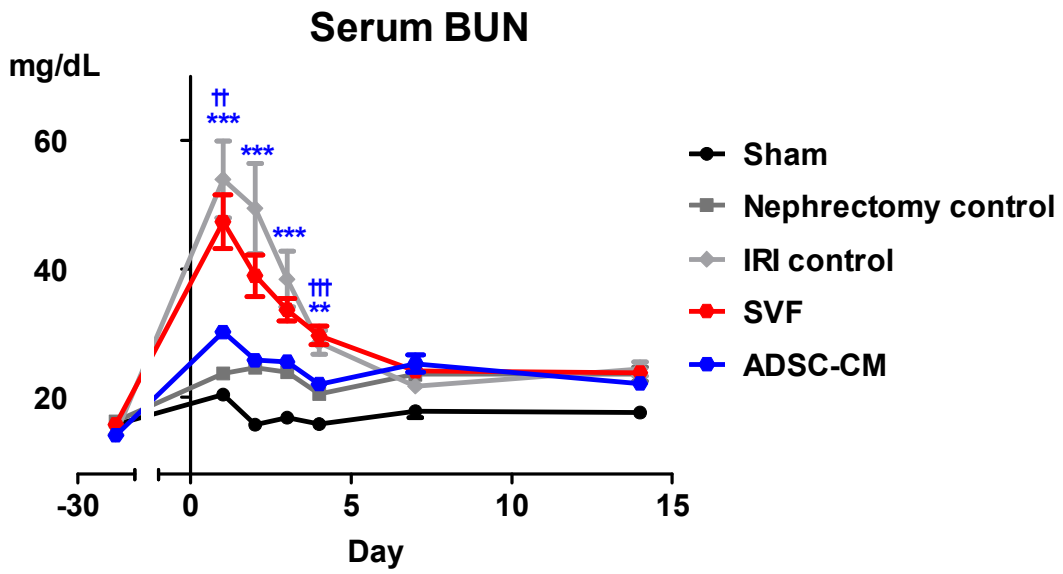
Serum BUN
mg/dL
60
40
20
-30
0
5
10
15
Day
Sham
Nephrectomy control
IRI control
SVF
ADSC-CM

B.

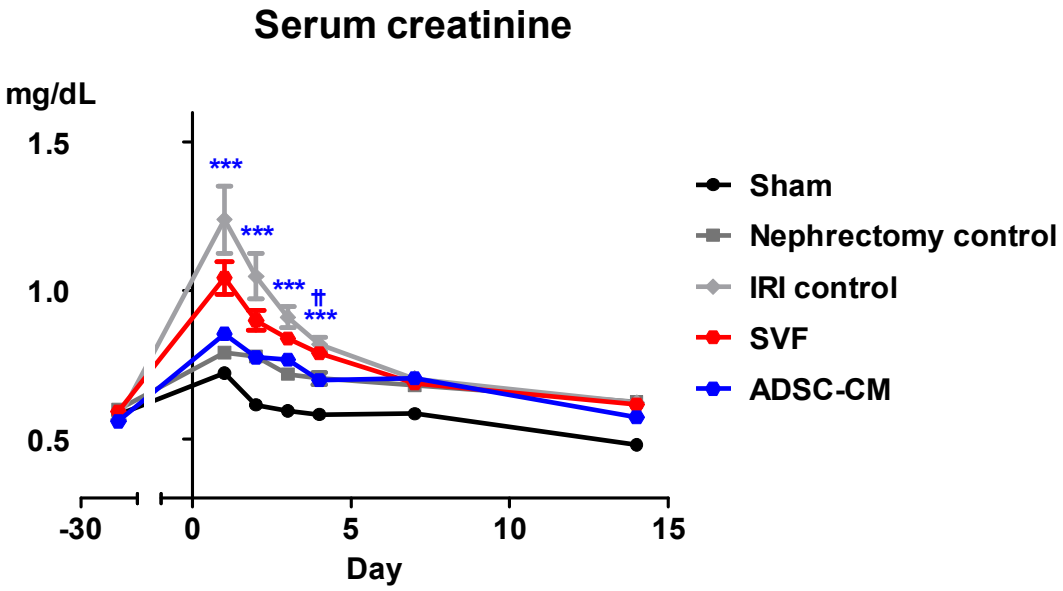
Serum creatinine
mg/dL
1.5
1.0
0.5
-30
0
5
10
15
Day
Sham
Nephrectomy control
IRI control
SVF
ADSC-CM

C.

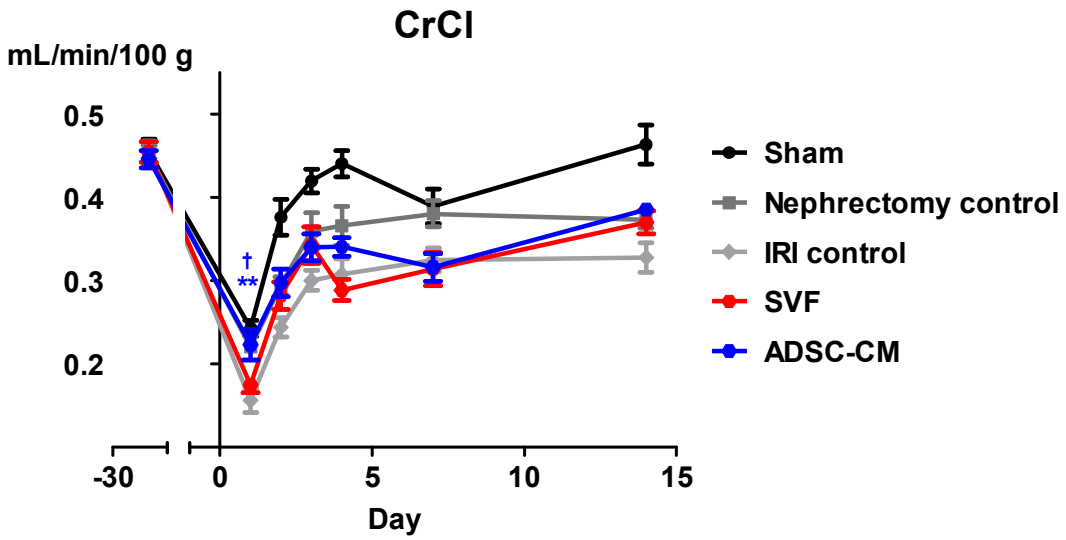

Figure 4. Effects of SVF and ADSC-CM on renal function. (A) Changes in serum BUN, (B) serum creatinine, and (C) CrCl of each group during the experiment. Blue-colored stars indicate statistically significant differences in the ADSC-CM group compared with the IRI control group; **, $p < 0.01$; ***, $p < 0.001$. Blue-colored crosses indicate statistically significant differences between the SVF and ADSC-CM groups; †, $p < 0.05$; ††, $p < 0.01$; †††, $p < 0.001$. Three times per rat, ten rats per group, but nine rats in the ADSC-CM group. Abbreviations: BUN, blood urea nitrogen; CrCl, creatinine clearance; IRI, ischemia-reperfusion injury; SVF, stromal vascular fraction; ADSC-CM, adipose-derived stem cell-conditioned medium.

Renal Index and Gross Pictures of Harvested Kidneys

The renal index of the harvested kidneys was significantly increased in all the groups compared with the sham group (Figure 5A). No gross differences in kidney cross-sections were observed (Figure 5B).

A.

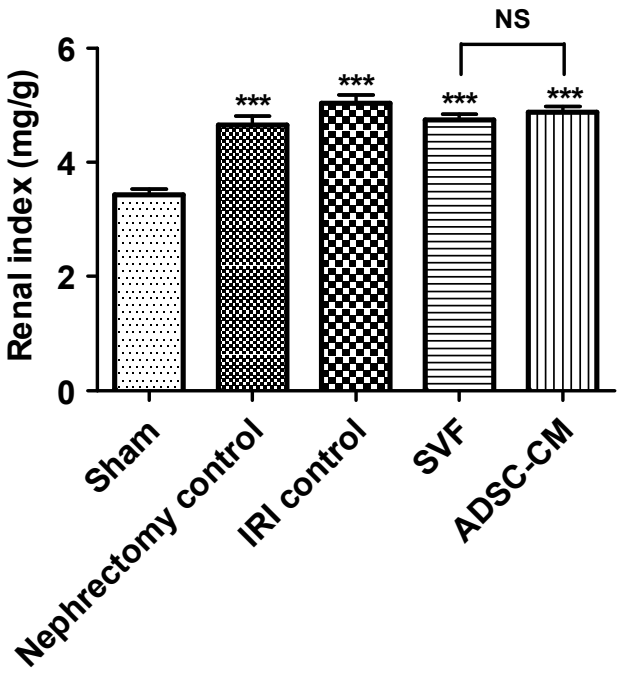

B.

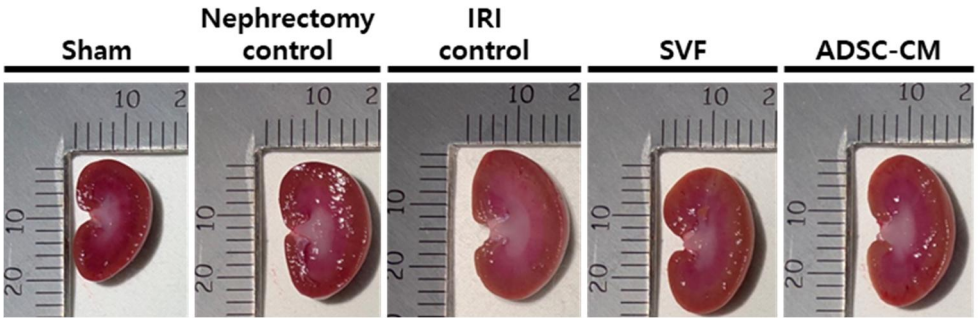

Figure 5. (A) Renal index of left kidneys after harvest. ***, $p < 0.001$ compared with the sham group. NS, $p > 0.05$ between the SVF and ADSC-CM groups. (B) Representative pictures of cross-sectioned left kidneys. Ten rats per group, but nine rats in the ADSC-CM group.

Abbreviations: NS, not significant; IRI, ischemia-reperfusion injury; SVF, stromal vascular fraction; ADSC-CM, adipose-derived stem cell-conditioned medium.

Histopathological Score and Collagen Content of Kidney Tissue

Histopathological scores were significantly higher in the IRI control group than in the sham and nephrectomy control groups. There were no significant differences in histopathological scores among the IRI control, SVF, and ADSC-CM groups (Figure 6).

Sirius red staining revealed that collagen content was significantly higher in the IRI control group than in the sham and nephrectomy control groups in both cortex and medulla. Collagen content was significantly lower in the SVF and ADSC-CM groups than in the IRI control group in both cortex and medulla. It was significantly lower in the SVF group than in the ADSC-CM group in both cortex and medulla (Figure 7).

A.

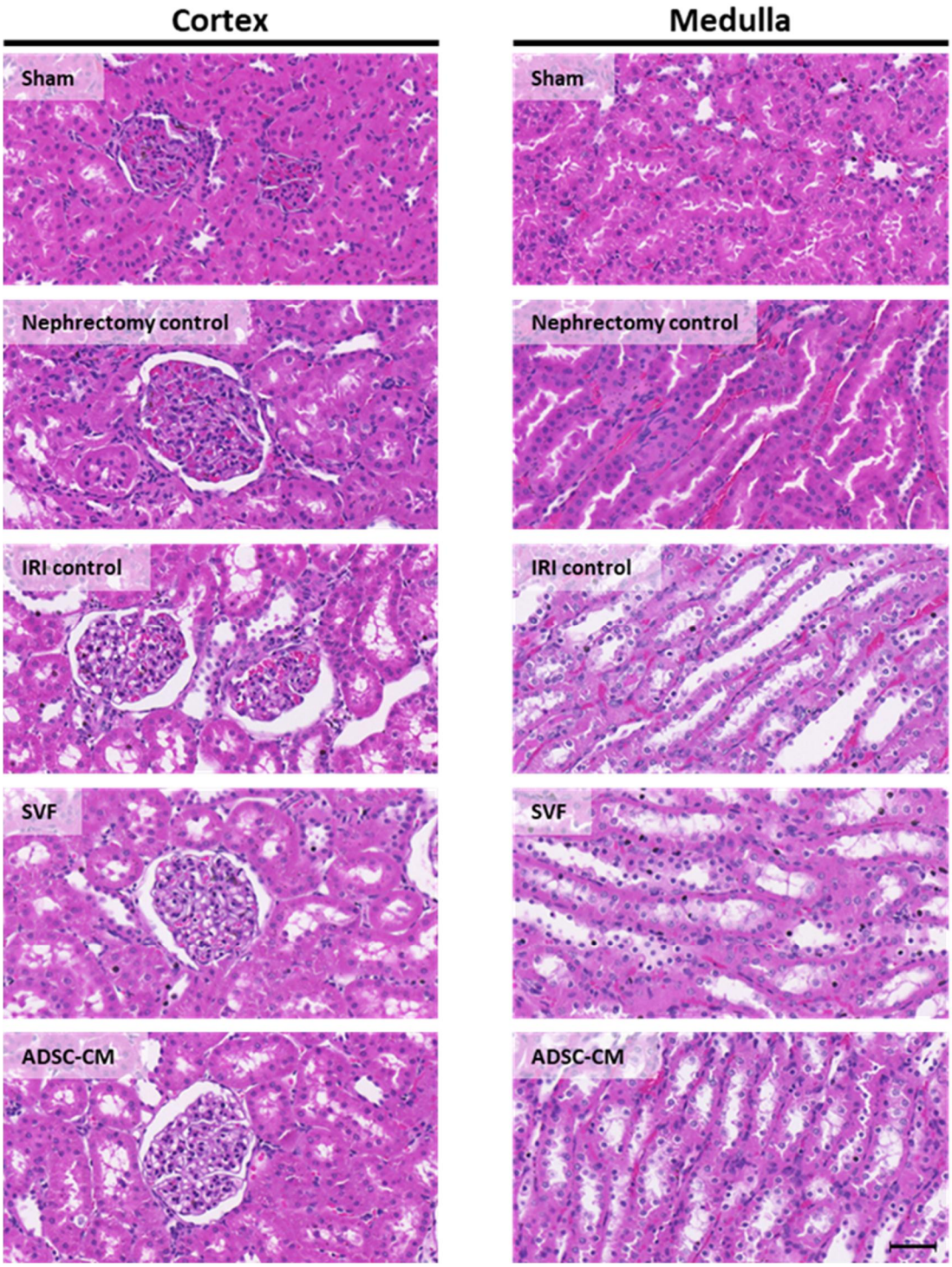
Cortex
Medulla
Sham
Sham
Nephrectomy control
Nephrectomy control
IRI control
IRI control
SVF
SVF
ADSC-CM
ADSC-CM

B.

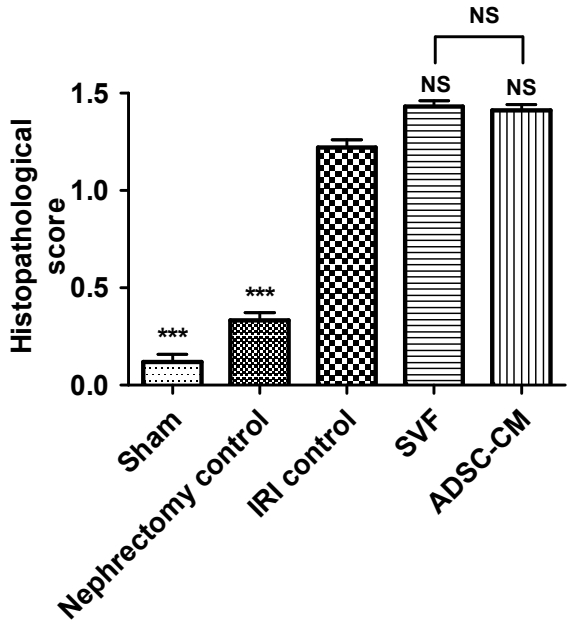

Figure 6. Hematoxylin and eosin staining of kidney tissue. (A) Representative photomicrographs of cortex and medulla. (B) Histopathological score in random non-overlapping fields. Magnification ×40. Scale bar 50 μm. NS, $p > 0.05$; ***, $p < 0.001$ compared with the IRI control group. NS, $p > 0.05$ between the SVF and ADSC-CM groups. Ten fields per rat, ten rats per group, but nine rats in the ADSC-CM group.

Abbreviations: NS, not significant; IRI, ischemia-reperfusion injury; SVF, stromal vascular fraction; ADSC-CM, adipose-derived stem cell-conditioned medium.

A.

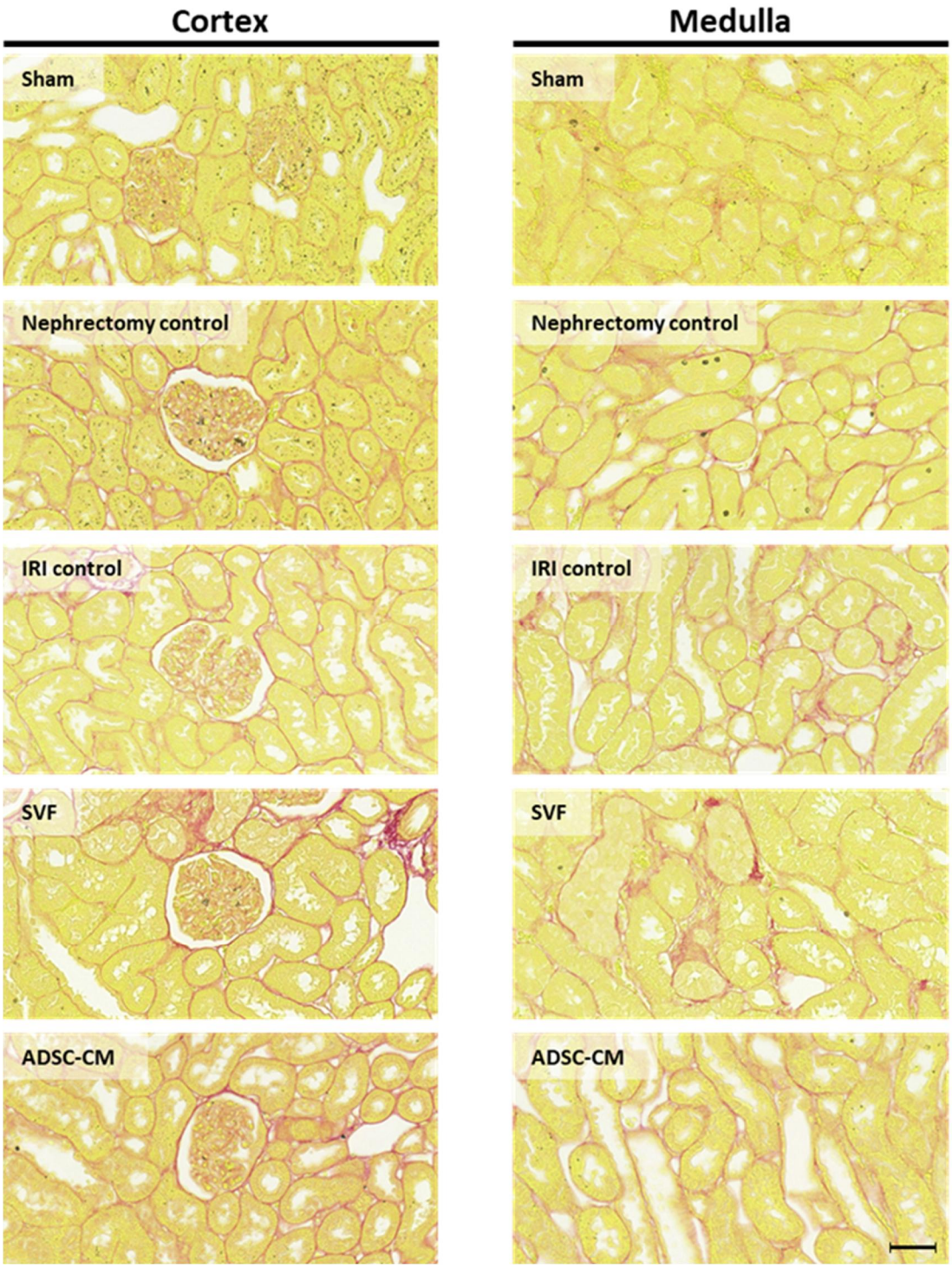
Cortex
Medulla
Sham
Sham
Nephrectomy control
Nephrectomy control
IRI control
IRI control
SVF
SVF
ADSC-CM
ADSC-CM

B.

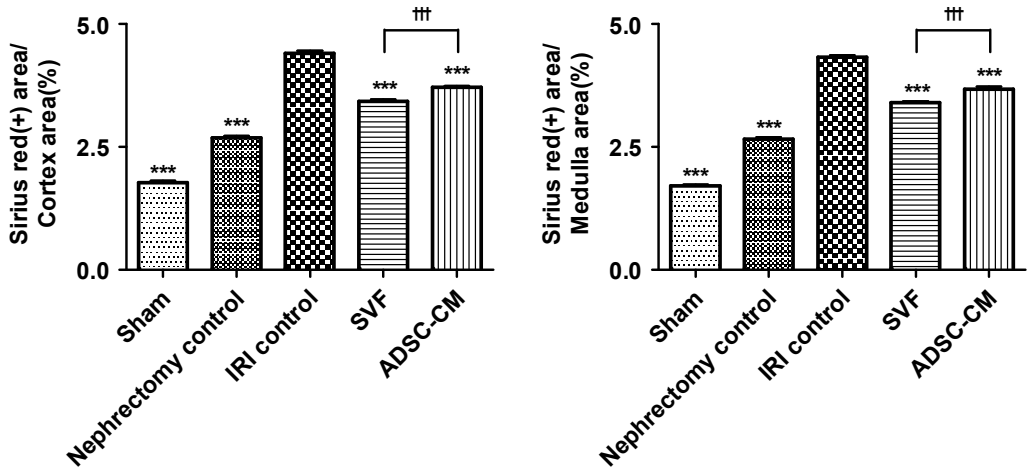

Figure 7. Sirius red staining of kidney tissue. (A) Representative photomicrographs of cortex and medulla. (B) The ratio of collagen-positive stained areas to random cortex and medulla areas. Magnification ×40. Scale bar 50 μm. ***, $p < 0.001$ compared with the IRI control group. †††, $p < 0.001$ between the SVF and ADSC-CM groups. Four fields per rat, ten rats per group, but nine rats in the ADSC-CM group.

Abbreviations: IRI, ischemia-reperfusion injury; SVF, stromal vascular fraction; ADSC-CM, adipose-derived stem cell-conditioned medium.

Apoptosis and Proliferation Markers of Kidney Tissue

The TUNEL assay revealed a significant increase in apoptosis in the cortex and medulla in the IRI control group compared with the sham and nephrectomy control groups. Apoptosis in the cortex and medulla was significantly decreased in the SVF and ADSC-CM groups compared with the IRI control group. Apoptosis in the cortex and medulla was significantly decreased in the SVF group than in the ADSC-CM group (Figure 8).

Ki67 staining revealed a significant increase in proliferation in the cortex and medulla in the IRI control group compared with the sham and nephrectomy control groups. Proliferation in the cortex and medulla was significantly increased in the SVF and ADSC-CM groups compared with the IRI control group. Proliferation in the cortex and medulla was significantly increased in the SVF group than in the ADSC-CM group (Figure 9).

A.

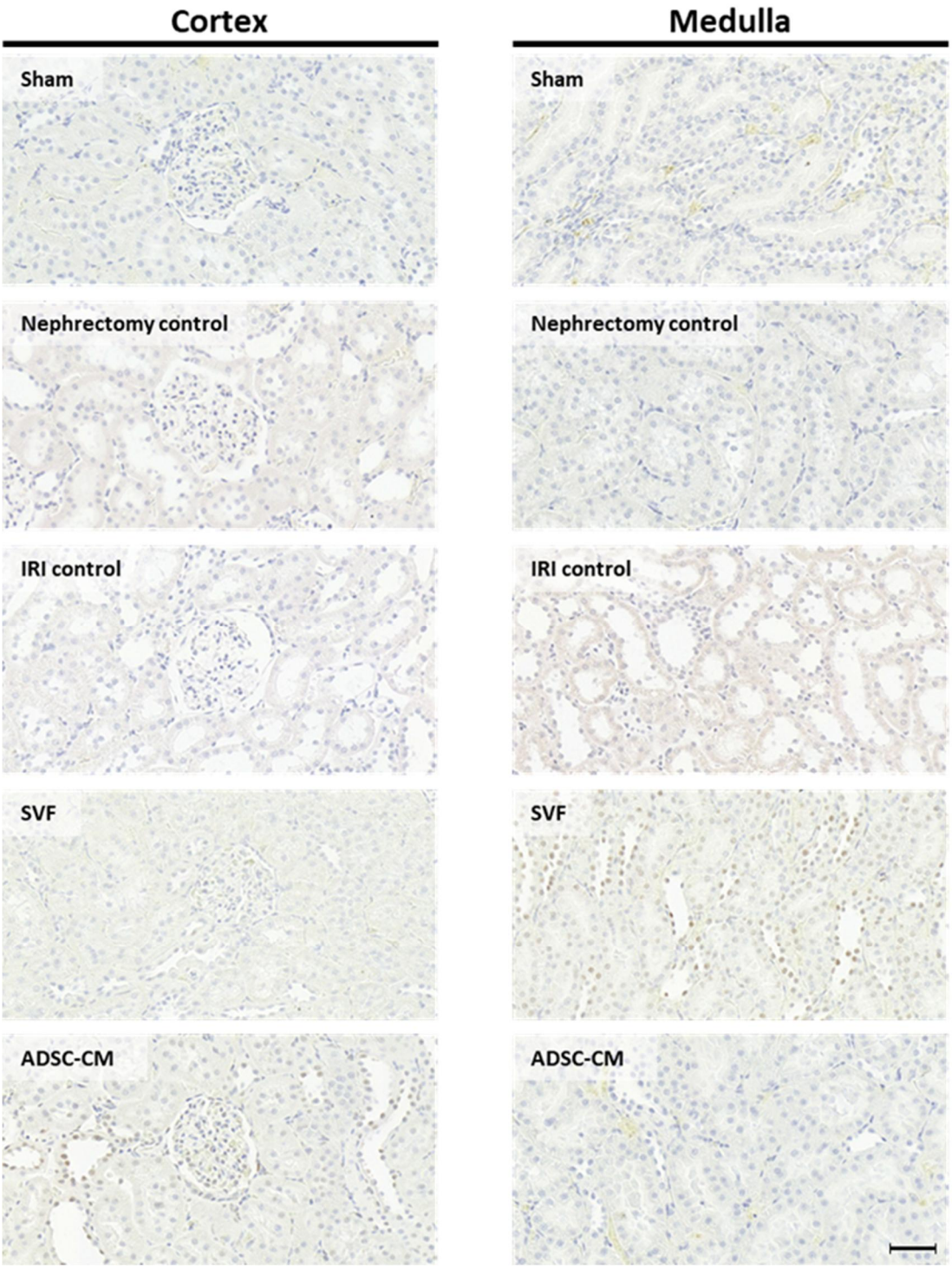
Cortex
Medulla
Sham
Sham
Nephrectomy control
Nephrectomy control
IRI control
IRI control
SVF
SVF
ADSC-CM
ADSC-CM

B.

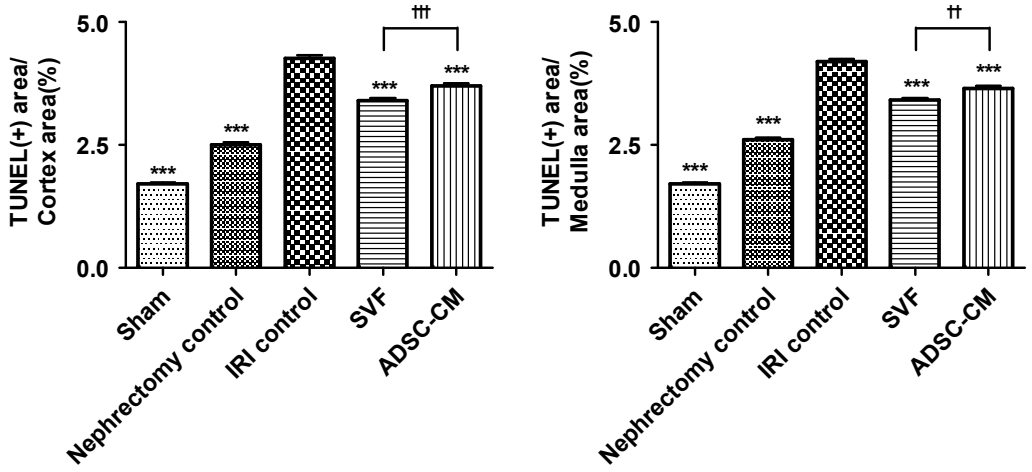

Figure 8. TUNEL assay of kidney tissue. (A) Representative photomicrographs of cortex and medulla. (B) The ratio of TUNEL-positive stained areas to random cortex and medulla areas. Magnification ×40. Scale bar 50 μm. ***, $p < 0.001$ compared with the IRI control group. ††, $p < 0.01$; †††, $p < 0.001$ between the SVF and ADSC-CM groups. Four fields per rat, ten rats per group, but nine rats in the ADSC-CM group.

Abbreviations: TUNEL, terminal deoxynucleotidyl transferase dUTP nick end labeling; IRI, ischemia-reperfusion injury; SVF, stromal vascular fraction; ADSC-CM, adipose-derived stem cell-conditioned medium.

A.

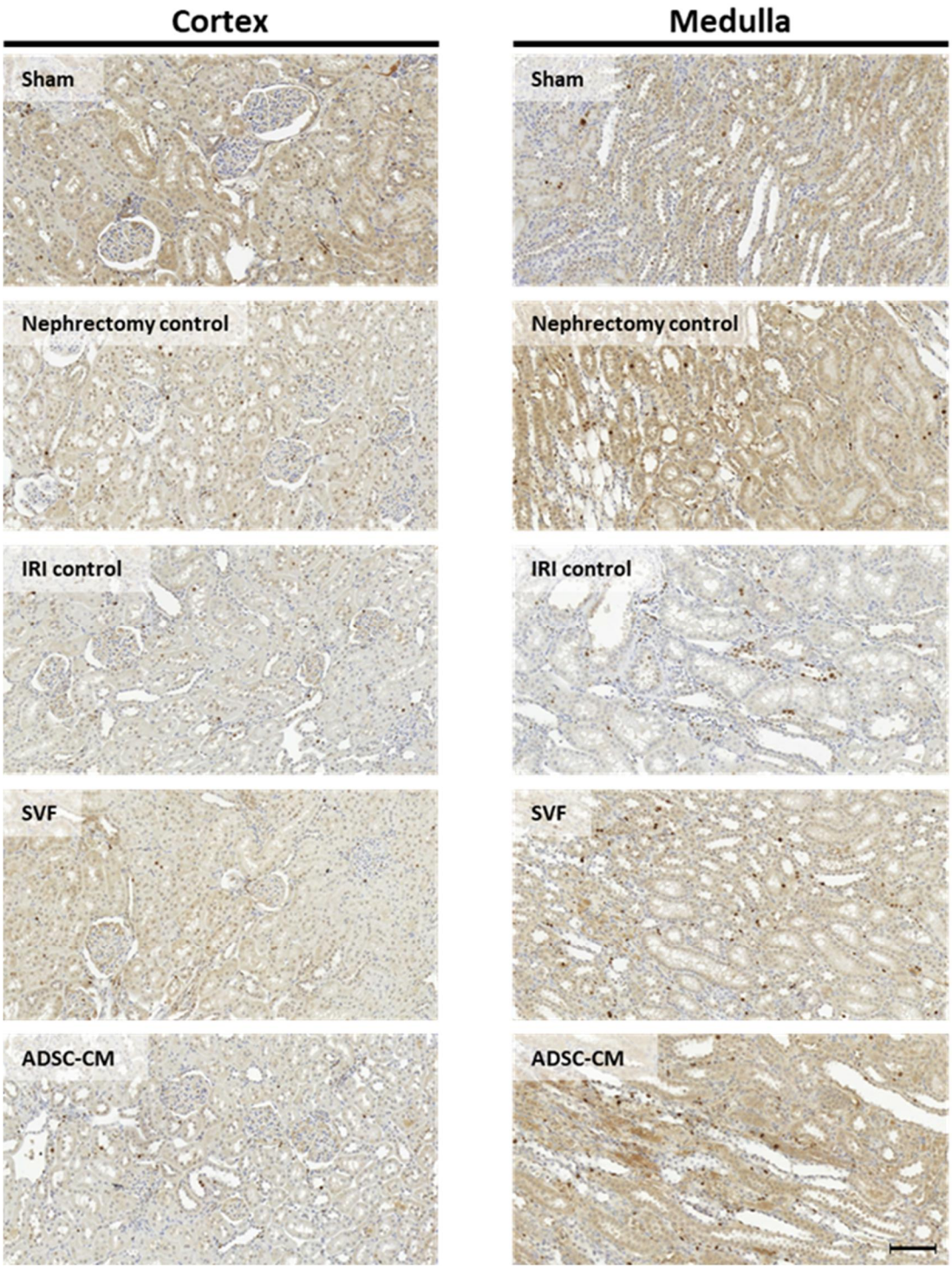
Cortex
Medulla
Sham
Sham
Nephrectomy control
Nephrectomy control
IRI control
IRI control
SVF
SVF
ADSC-CM
ADSC-CM

B.

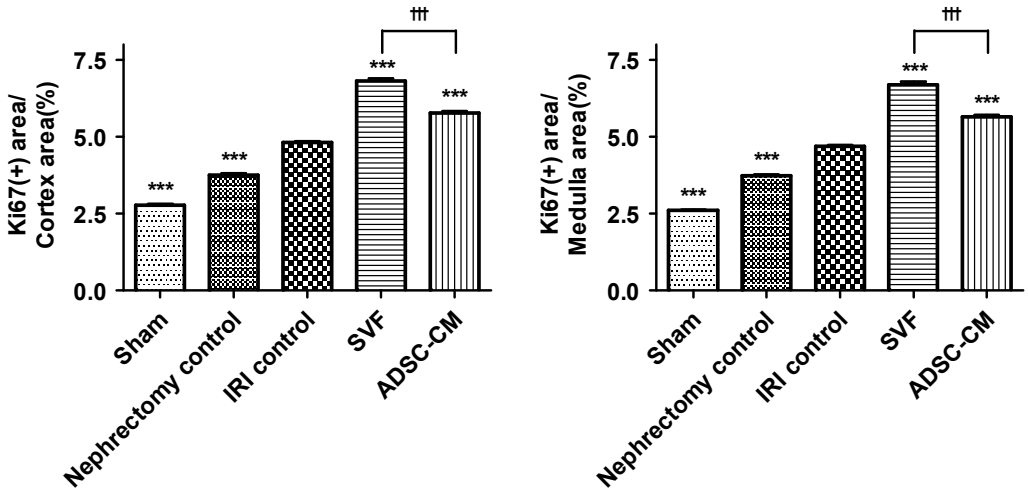

Figure 9. Ki67 immunohistochemistry of kidney tissue. (A) Representative photomicrographs of cortex and medulla. (B) The ratio of Ki67-positive stained areas to random cortex and medulla areas. Magnification ×40. Scale bar 50 μm. ***, $p < 0.001$ compared with the IRI control group. †††, $p < 0.001$ between the SVF and ADSC-CM groups. Four fields per rat, ten rats per group, but nine rats in the ADSC-CM group.

Abbreviations: IRI, ischemia-reperfusion injury; SVF, stromal vascular fraction; ADSC-CM, adipose-derived stem cell-conditioned medium.

Anti-oxidative Markers of Kidney Tissue

The GR-positive areas in the cortex and medulla were significantly higher in the IRI control group than in the sham and nephrectomy control groups. The GR-positive staining was significantly higher in the SVF and ADSC-CM groups than in the IRI control group in the cortex and medulla. The GR-positive staining was significantly higher in the SVF group than in the ADSC-CM group in the cortex and medulla (Figure 10).

The GPx-positive areas in the cortex and medulla were significantly higher in the IRI control group than in the sham and nephrectomy control groups. The GPx-positive staining was significantly higher in the SVF and ADSC-CM groups than in the IRI control group in the cortex and medulla. The GPx-positive staining was significantly higher in the SVF group than in the ADSC-CM group in the cortex and medulla (Figure 11).

A.

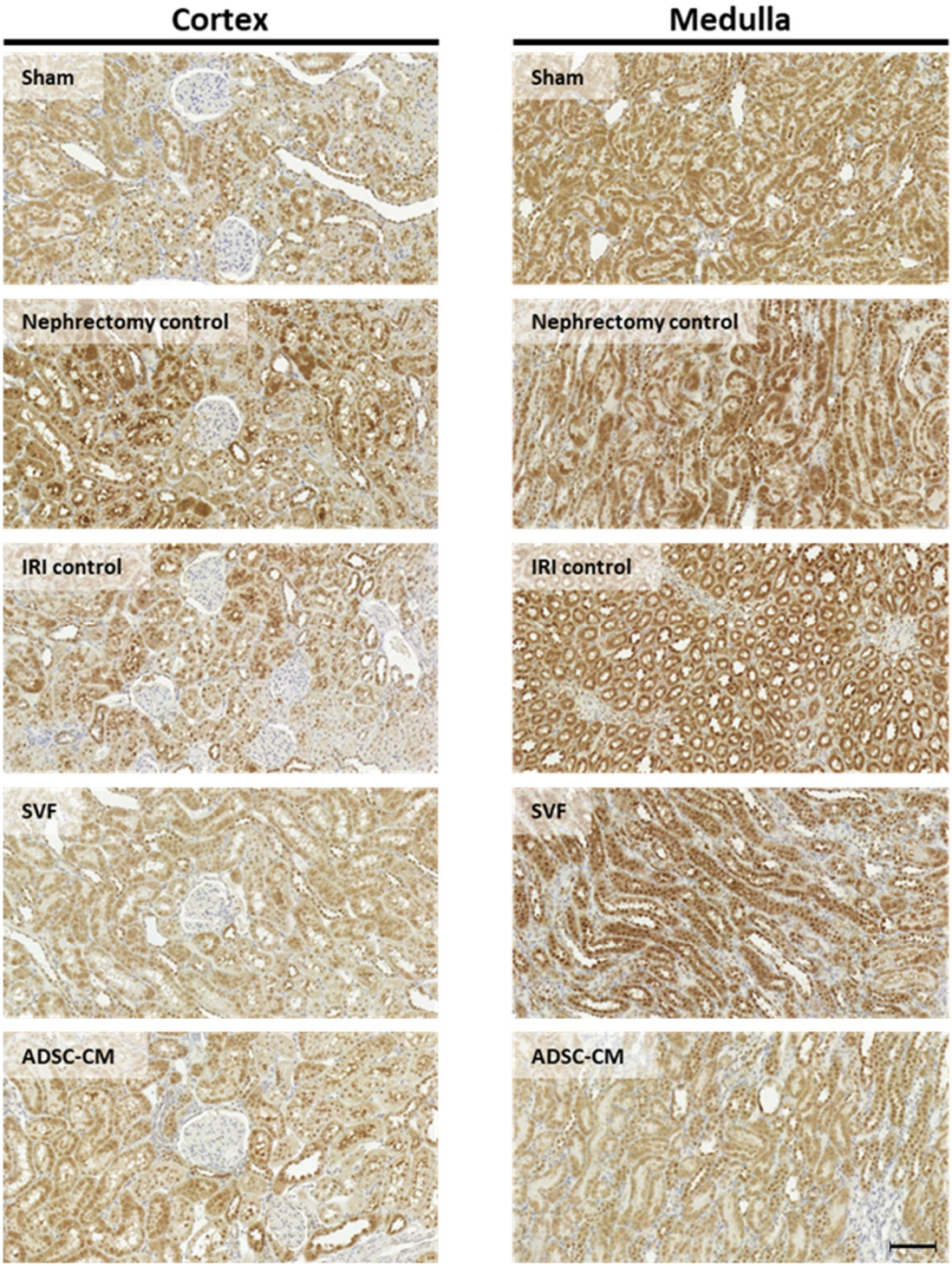
Cortex
Medulla
Sham
Sham
Nephrectomy control
Nephrectomy control
IRI control
IRI control
SVF
SVF
ADSC-CM
ADSC-CM

B.

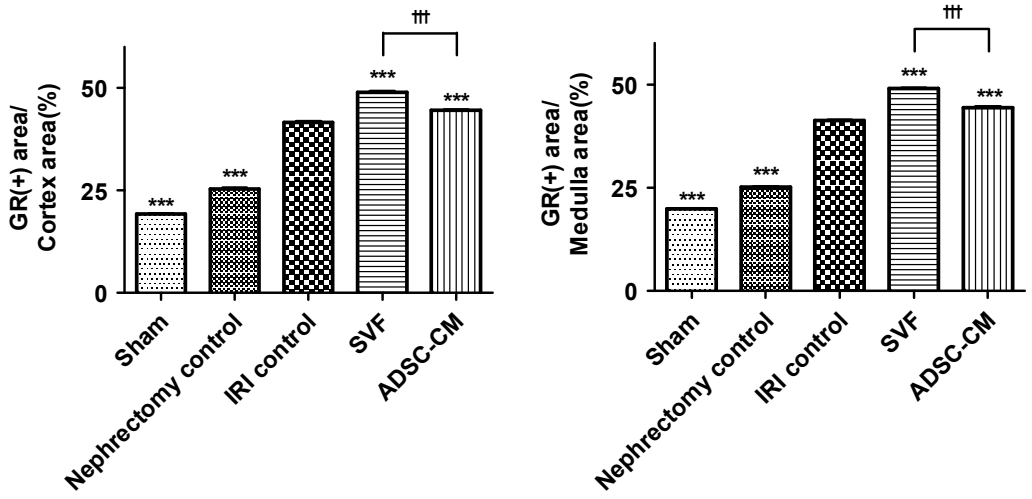

Figure 10. GR immunohistochemistry of kidney tissue. (A) Representative photomicrographs of cortex and medulla. (B) The ratio of GR-positive stained areas to the random cortex and medulla areas. Magnification ×40. Scale bar 50 μm. ***, $p < 0.001$ compared with the IRI control group. †††, $p < 0.001$ between the SVF and ADSC-CM groups. Four fields per rat, ten rats per group, but nine rats in the ADSC-CM group.

Abbreviations: GR, glutathione reductase; IRI, ischemia-reperfusion injury; SVF, stromal vascular fraction; ADSC-CM, adipose-derived stem cell-conditioned medium.

A.

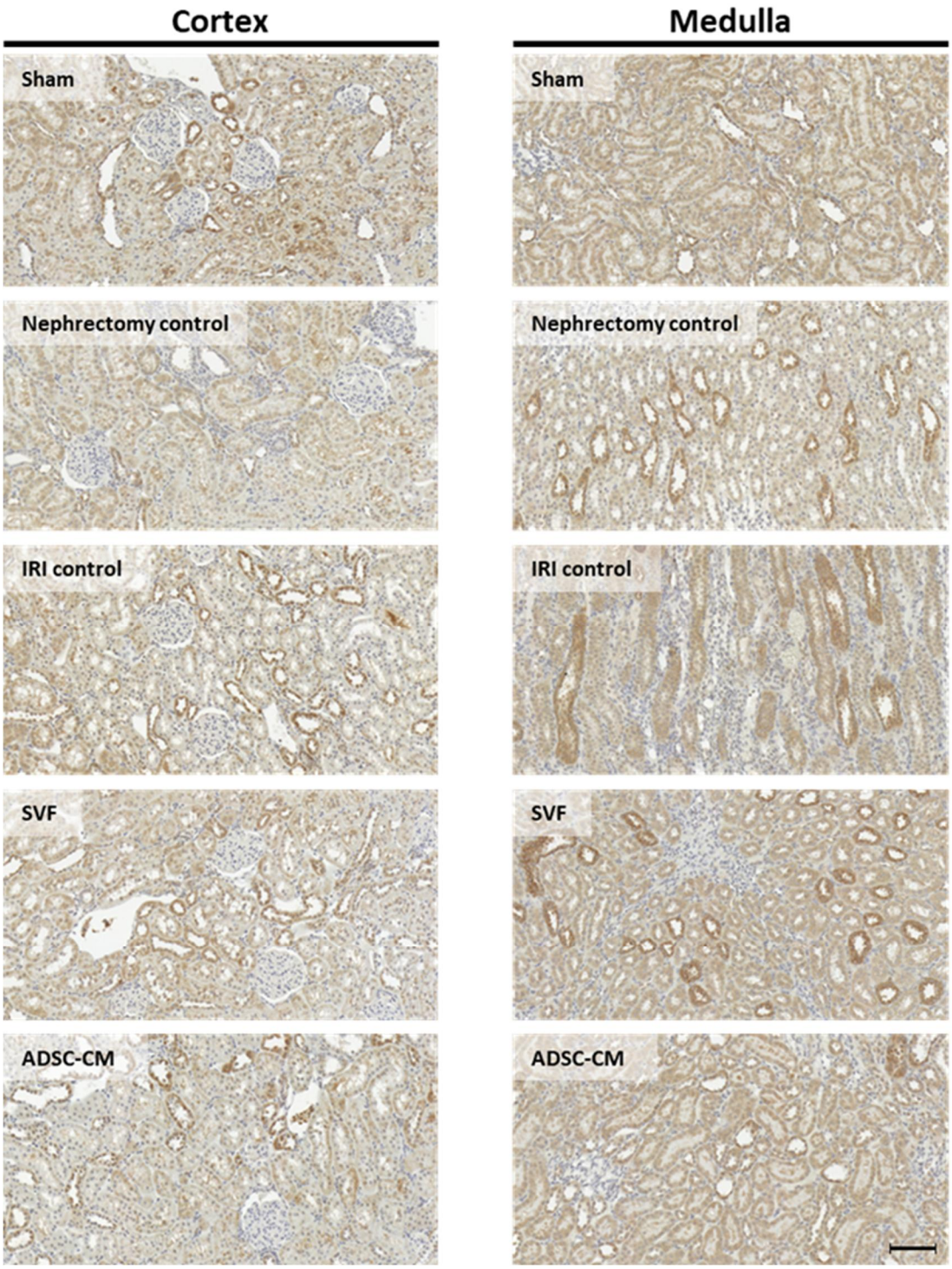
Cortex
Medulla
Sham
Sham
Nephrectomy control
Nephrectomy control
IRI control
IRI control
SVF
SVF
ADSC-CM
ADSC-CM

B.

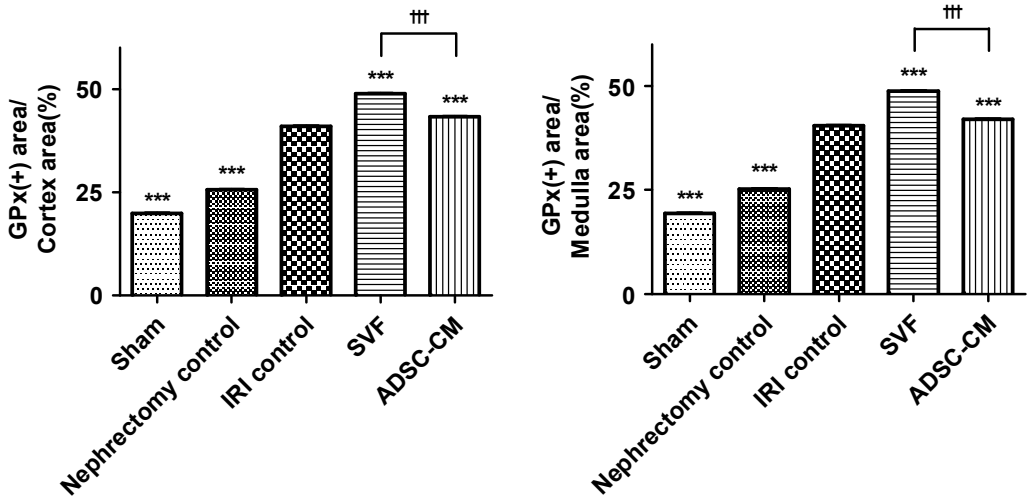

Figure 11. GPx immunohistochemistry of kidney tissues. (A) Representative photomicrographs of cortex and medulla. (B) The ratio of GPx-positive stained areas to random cortex and medulla areas. Magnification ×40. Scale bar 50 μm. ***, $p < 0.001$ compared with the IRI control group. †††, $p < 0.001$ between the SVF and ADSC-CM groups. Four fields per rat, ten rats per group, but nine rats in the ADSC-CM group.

Abbreviations: GPx, glutathione peroxidase; IRI, ischemia-reperfusion injury; SVF, stromal vascular fraction; ADSC-CM, adipose-derived stem cell-conditioned medium.

SVF Localization with CM-Di1

Two weeks after injection, all treatment groups showed no CM-DiI-labeled SVF in the kidney (Figure 12).

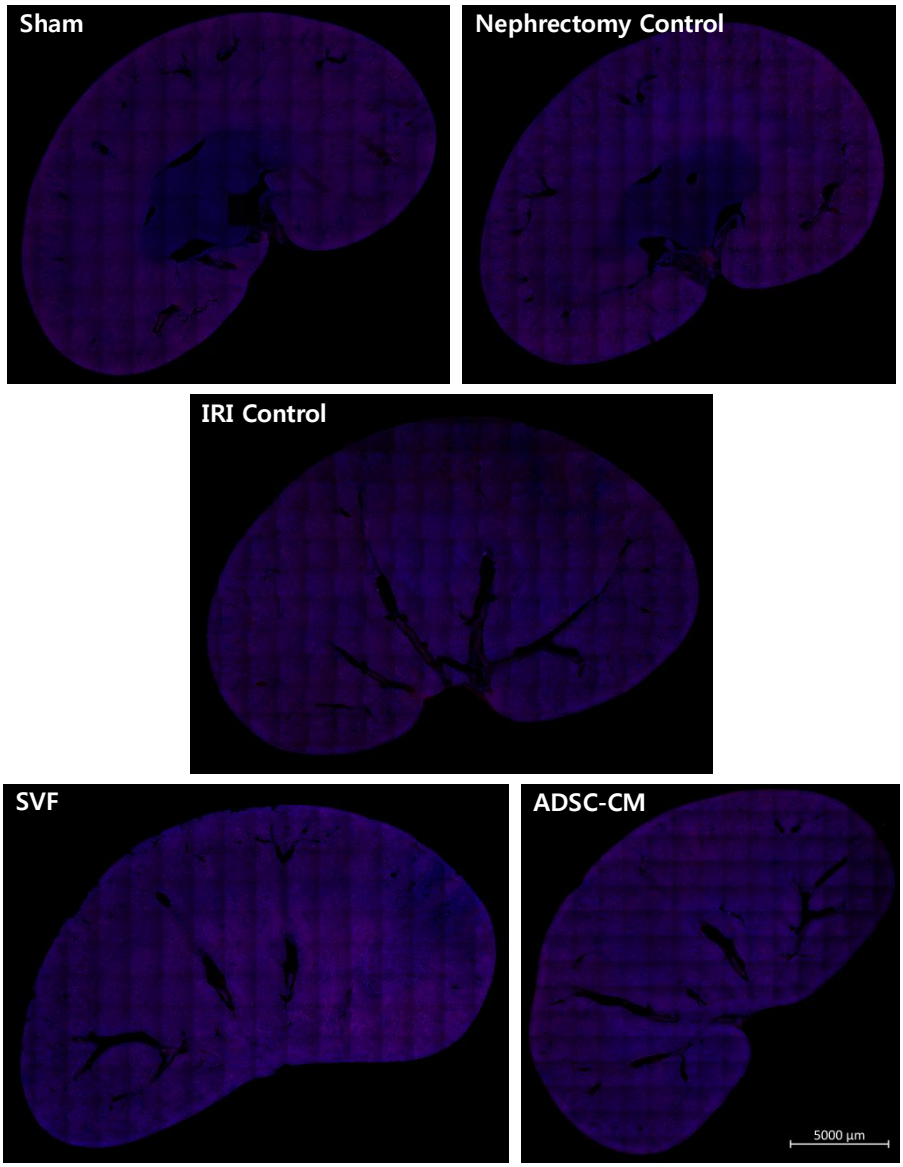

Figure 12. Determination of CM-DiI-labeled SVF. CM-DiI-labeled SVF was observed by a fluorescent microscope.

Abbreviations: IRI, ischemia-reperfusion injury; SVF, stromal vascular fraction; ADSC-CM, adipose-derived stem cell-conditioned medium.

DISCUSSION

Preclinical and clinical studies have investigated the effects of MSC in the treatment of AKI.[6,7] However, MSC treatment has several limitations, including tumorigenicity,[8] microbiological contamination,[9] putative profibrogenic potential,[10] and heterogeneity and functional diversity.[11] Preclinical studies using adipose tissue-derived SVF to treat AKI have increased because of the limitations in MSC treatments.[12-16] However, SVF also has several limitations, including decreased cell viability during freezing and thawing, immune rejection when using allogeneic cells, and putative thrombogenic potential.[18] In order to compensate for the shortcomings in cell-based therapies including MSC and SVF, CM therapy uses trophic factors and cytokines secreted from cells and has become increasingly attractive for the treatment of AKI.[19] The CM which stem cells were cultured in contains many secretions called secretomes, microvesicles, or exosomes secreted from stem cells.[35] Several preclinical studies have focused using stem cell-CM to treat AKI induced by cisplatin, renal IRI, and gentamicin.[20-22] However, the studies comparing stem cells with their CM have questioned the effectiveness of stem cell-CM.[23,25]

Meanwhile, various methods, including culture conditions, drugs, and external stimuli, have been studied to attain more of the valuable secretions from stem cells.[26,35-40] One interesting method is stem cells cultured in hypoxic conditions and produces more angiogenic factors than in normoxic conditions.[41-43] There are several methods to induce hypoxic culture conditions, including gas-controlled incubators, glove boxes, and biochemical induction of pseudo-hypoxic states.[44] However, these methods require purchasing expensive equipment or treatment with drugs that must be removed later and cause cell damage. Several researchers have found that cells at the core of the spheroid are naturally exposed to mild hypoxia and limited nutrient diffusion.[45] This method can induce hypoxic culture conditions cheaply and easily compared with other methods. The 3D Petri

Dish® is a natural, scaffold-free 3D spheroid culture system to maximize cell-to-cell interactions. We found that human BMSC spheroids cultured using the 3D Petri Dish® showed a marked increase in cytokine secretion compared with the secretions in a 2D culture.[30)]

We previously reported that renal function is effectively protected from renal IRI-induced AKI through renal parenchymal injections of SVF, which enhanced the anti-fibrotic, anti-apoptotic, and anti-oxidative effects.[17)] This led to this study comparing autologous SVF with ADSC-CM prepared using a 3D spheroid culture system and injecting via the renal parenchymal route to explore the effectiveness of treating renal IRI-induced AKI.

We found that renal parenchymal injections of ADSC-CM effectively restored renal function from renal IRI-induced AKI in terms of renal functions and histological examinations except histopathological scores. Moreover, ADSC-CM was superior to SVF in terms of serum BUN, creatinine, and CrCl until 4 days after IRI. However, the differences disappeared 7 days after IRI induction, and histological examinations showed more positive findings in the SVF group than in the ADSC-CM group.

Tarng et al.[21)] examined whether induced pluripotent stem cell (iPSC)-CM via intraperitoneal administration exhibited a systemic effect against renal IRI-induced AKI. They found that administration of iPSC-CM significantly improved renal function and survival rates in rats and protected tubular cells against apoptosis. The level of serum BUN and creatinine were significantly lower in iPSC-CM-treated rats than in normal control medium (NM)-treated rats 2 days after IRI. Similar to our study, no differences in serum BUN and creatinine levels were observed between the iPSC-CM- and NM-treated rats 7 days after IRI. Meanwhile, about 70% of PBS or NM-treated rats died within 7 days, whereas the mortality rate of iPSC-CM-treated rats was 30%. However, in our study, there was no mortality related to the AKI. The lack of mortality of our study might be attributed to our shorter clamping time of the renal artery than in their study (40 min vs. 45 min).

Similar reno-protective effects of stem cell-CM were also confirmed in other types of AKI models. Bi et al.[20] found that mice with intraperitoneal administration of bone marrow–derived MSC (BMSC)-CM or ADSC-CM limited the renal injury, increased survival, and diminished tubular cell apoptosis after cisplatin injection. The levels of serum BUN were markedly improved in both BMSC-CM and ADSC-CM-treated mice on days 3 and 5 after cisplatin injection. Six of the 15 mice in the cisplatin control group had died by day 6, whereas no mice died in either CM-treated group. Abedi et al.[22] found that intraperitoneal administration of human BMSC-CM in a gentamicin-induced AKI rat model showed relative improvement in some indicators of tissue injury. Although human BMSC-CM did not improve serum BUN and creatinine levels in all treatment groups, BMSC-CM injection one day before gentamicin injection diminished tissue damage. The authors assumed that the injection time of human BMSC-CM had a role in injury recovery. Similarly, our previous study found that injections 2 days before or concurrently with IRI had beneficial effects, whereas injections 2 days later did not have any benefit.[31]

Meanwhile, some researchers have compared the effects of stem cells with their CM. Abouelkheir et al.[24] compared the efficacy of subcapsular injections of BMSC with intraperitoneal injections of BMSC-CM in a model of cisplatin-induced AKI. Both BMSC and BMSC-CM equally ameliorated kidney function deteriorations, tubular cell apoptosis, and reduced interstitial fibrosis after 2 months. However, adipocytes and osteoblast-like cells were detected at the BMSC injection site. The authors concluded that BMSC-CM might be an acceptable alternative to BMSC therapy as it attained comparable efficacy without the development of unwanted cells.

However, other researchers have questioned the effectiveness of CM. Abd El Zaher F et al.[21] compared the effect of intravenous injections of BMSC versus BMSC-CM in minimizing cisplatin-induced AKI damage. The BMSC injection showed noticeable improvement of renal structures with a significant increase in Proliferating Cell Nuclear

Antigen, but the BMSC-CM was less effective. Xing et al.[23] investigated the therapeutic potential of BMSC and BMSC-CM intravenously administered 1 day after IRI-induced AKI and found that BMSC injections improved renal function and histological alterations, leading to significantly reduced mortality. Although BMSC-CM contained proangiogenic factors, including hepatocyte growth factor, vascular endothelial growth factor-A, and insulin-like growth factor-1, beneficial effects were not detected.

Unlike their study, our study demonstrated that ADSC-CM was superior to SVF in terms of serum BUN, creatinine, and CrCl in the early phase after renal IRI. There are possible explanations for the differences between the previous two studies and ours. First, in both studies, BMSC and BMSC-CM were injected intravenously.[21,23] BMSC has a homing effect on the injured site; however, BMSC-CM does not display this property and may not effectively reach the injured site. In our study, the effective delivery to the injured site was possible by direct injection into the renal parenchyma. Second, ADSC-CM from our study may have contained more cytokines since we used a 3D spheroid culture system instead of a 2D culture system.[26,30] Finally, small molecular weight cytokines in the ADSC-CM diffused more effectively in the renal parenchyma than the SVF composed of heterogeneous cells. This may explain why the differences between ADSC-CM and SVF disappeared 7 days after IRI.

Our study had some limitations. First, the exact composition of the SVF and ADSC-CM was not investigated. Second, the rats were followed for only 2 weeks. Longer studies are needed to determine whether SVF and ADSC-CM can prevent progression to chronic kidney disease. Zhou et al.[46] reported that preischemic administration of SVF reduced serum creatinine levels 6 months after IRI-induced AKI, inhibited renal fibrosis, and slowed the progression of chronic kidney disease. Abouelkheir et al.[24] reported that intraperitoneal injection of BMSC-CM reduced interstitial fibrosis 2 months after cisplatin-induced AKI. Third, the rats were only injected once with a fixed-dose applied concurrently with the

induction of IRI. As mentioned above, since ADSC-CM spreads quickly, there may be a need for repeated or divided dosing. However, ADSC-CM is suitable for repeated or divided dosing because, unlike SVF, it can be frozen without significantly compromising the cell viability. Lastly, there are reports that female rats were more resistant to IRI than male rats, which raises questions about whether the results from male-only studies can be equally applied to females.[47] Nevertheless, the findings from our study suggest that ADSC-CM holds a promise as a safe therapeutic approach for the treatment of predictable injuries that might be induced by kidney surgeries and avoid the various adverse effects of cell-based therapy.

CONCLUSIONS

Our study suggests that renal function is effectively rescued after IRI through renal parenchymal injections of ADSC-CM by enhanced anti-fibrotic, anti-apoptotic, and anti-oxidative effects. The ADSC-CM was superior to SVF in terms of serum BUN, creatinine, and CrCl in the early phase after renal IRI, but the difference disappeared 7 days after IRI.

ACKNOWLEDGEMENTS

This work was supported by the National Research Foundation of Korea (NRF) grant funded by the Korea government (MSIT) (2019R1H1A1079751).

REFERENCES

1. Webb S, Dobb G. "ARF, ATN or AKI? It's now acute kidney injury". Anaesth Intensive Care. 2007 Dec;35(6):843–4.
2. Mehta RL, Cerdá J, Burdmann EA, Tonelli M, García-García G, Jha V, Susantitaphong P, Rocco M, Vanholder R, Sever MS, Cruz D, Jaber B, Lameire NH, Lombardi R, Lewington A, Feehally J, Finkelstein F, Levin N, Pannu N, Thomas B, Aronoff-Spencer E, Remuzzi G. International Society of Nephrology's 0by25 initiative for acute kidney injury (zero preventable deaths by 2025): a human rights case for nephrology. Lancet 2015 Jun 27;385(9987):2616–43.
3. Case J, Khan S, Khalid R, Khan A. Epidemiology of acute kidney injury in the intensive care unit. Crit Care Res Pract 2013;2013:479730.
4. Bonventre JV, Weinberg JM. Recent advances in the pathophysiology of ischemic acute renal failure. J Am Soc Nephrol. 2003 Aug;14(8):2199–210.
5. Malek M, Nematbakhsh M. Renal ischemia/reperfusion injury; from pathophysiology to treatment. J Renal Inj Prev. 2015 Jun 1;4(2):20–7.
6. Wang Y, He J, Pei X, Zhao W. Systematic review and meta-analysis of mesenchymal stem/stromal cells therapy for impaired renal function in small animal models. Nephrology (Carlton). 2013 Mar;18(3):201–8.
7. Sávio-Silva C, Soinski-Sousa PE, Balby-Rocha MTA, Lira ÁO, Rangel ÉB. Mesenchymal stem cell therapy in acute kidney injury (AKI): review and perspectives. Rev Assoc Med Bras 2020 Jan 13;66 Suppl 1(Suppl 1):s45–s54.
8. Barkholt L, Flory E, Jekerle V, Lucas-Samuel S, Ahnert P, Bisset L, Büscher D, Fibbe W, Foussat A, Kwa M, Lantz O, Mačiulaitis R, Palomäki T, Schneider CK, Sensebé L, Tachdjian G, Tarte K, Tosca L, Salmikangas P. Risk of tumorigenicity in mesenchymal

stromal cell-based therapies--bridging scientific observations and regulatory viewpoints. Cytotherapy. 2013 Jul;15(7):753–9.

9. Cobo F, Cortés JL, Cabrera C, Nieto A, Concha A. Microbiological contamination in stem cell cultures. Cell Biol Int 2007 Sep;31(9):991–5.
10. Russo FP, Alison MR, Bigger BW, Amofah E, Florou A, Amin F, Bou-Gharios G, Jeffery R, Iredale JP, Forbes SJ. The bone marrow functionally contributes to liver fibrosis. Gastroenterology. 2006 May;130(6):1807–21.
11. McLeod CM, Mauck RL. On the origin and impact of mesenchymal stem cell heterogeneity: new insights and emerging tools for single cell analysis. Eur Cell Mater. 2017 Oct 27;34:217–31.
12. Feng Z, Ting J, Alfonso Z, Strem BM, Fraser JK, Rutenberg J, Kuo HC, Pinkernell K. Fresh and cryopreserved, uncultured adipose tissue-derived stem and regenerative cells ameliorate ischemia-reperfusion-induced acute kidney injury. Nephrol Dial Transplant. 2010 Dec;25(12):3874–84.
13. Yasuda K, Ozaki T, Saka Y, Yamamoto T, Gotoh M, Ito Y, Yuzawa Y, Matsuo S, Maruyama S. Autologous cell therapy for cisplatin-induced acute kidney injury by using non-expanded adipose tissue-derived cells. Cytotherapy. 2012 Oct;14(9):1089–100.
14. Zhou L, Xu L, Shen J, Song Q, Wu R, Ge Y, Xin H, Zhu J, Wu J, Jia R. Preischemic Administration of Nonexpanded Adipose Stromal Vascular Fraction Attenuates Acute Renal Ischemia/Reperfusion Injury and Fibrosis. Stem Cells Transl Med. 2016 Sep;5(9):1277–88.
15. Zhou L, Song Q, Shen J, Xu L, Xu Z, Wu R, Ge Y, Zhu J, Wu J, Dou Q, Jia R. Comparison of human adipose stromal vascular fraction and adiposederived mesenchymal stem cells for the attenuation of acute renal ischemia/ reperfusion injury. Sci Rep. 2017 Mar 9;7:44058.

16. Lee C, Jang MJ, Kim BH, Park JY, You D, Jeong IG, Hong JH, Kim CS. Recovery of renal function after administration of adipose-tissue-derived stromal vascular fraction in rat model of acute kidney injury induced by ischemia/reperfusion injury. Cell Tissue Res. 2017 Jun;368(3):603–13.

17. Aum J, Jang MJ, Kim YS, Kim BH, An DH, Han JH, Suh N, Kim CS, You D. Comparison of Stromal Vascular Fraction and Adipose-Derived Stem Cells for Protection of Renal Function in a Rodent Model of Ischemic Acute Kidney Injury. Stem Cells Int. 2022 May 6;2022:1379680.

18. Tatsumi K, Ohashi K, Matsubara Y, Kohori A, Ohno T, Kakidachi H, Horii A, Kanegae K, Utoh R, Iwata T, Okano T. Tissue factor triggers procoagulation in tran splanted mesenchymal stem cells leading to thromboembolism. Biochem Biophys Res Commun. 2013 Feb 8;431(2):203–9.

19. Sun DZ, Abelson B, Babbar P, Damaser MS. Harnessing the Mesenchymal Stem Cell Secretome for Regenerative Urology. Nat Rev Urol. 2019 Jun;16(6):363–75.

20. Bi B, Schmitt R, Israilova M, Nishio H, Cantley LG. Stromal cells protect against acute tubular injury via an endocrine effect. J Am Soc Nephrol. J Am Soc Nephrol. 2007 Sep;18(9):2486–96.

21. Tarng DC, Tseng WC, Lee PY, Chiou SH, Hsieh SL. Induced Pluripotent Stem Cell-Derived Conditioned Medium Attenuates Acute Kidney Injury by Downregulating the Oxidative Stress-Related Pathway in Ischemia-Reperfusion Rats. Cell Transplant. 2016;25(3):517–30.

22. Abedi A, Azarnia M, Zahvarehy MJ, Foroutan T, Golestani S. Effect of Different Times of Intraperitoneal Injections of Human Bone Marrow Mesenchymal Stem Cell Conditioned Medium on Gentamicin-Induced Acute Kidney Injury. Urol J. 2016 Jun 28;13(3):2707–16.

23. Xing L, Cui R, Peng L, Ma J, Chen X, Xie RJ, Li B. Mesenchymal stem cells, not conditioned medium, contribute to kidney repair after ischemia-reperfusion injury. Stem Cell Res Ther. 2014 Aug 21;5(4):101.

24. Abouelkheir M, ElTantawy DA, Saad MA, Abdelrahman KM, Sobh MA, Lotfy A, Sobh MA. Mesenchymal stem cells versus their conditioned medium in the treatment of cisplatin-induced acute kidney injury: evaluation of efficacy and cellular side effects. Int J Clin Exp Med. 2016;9(12):23222–34.

25. Abd El Zaher F, El Shawarby A, Hammouda G, Bahaa N. Role of Mesenchymal Stem Cells Versus their Conditioned Medium on Cisplatin-Induced Acute Kidney Injury in Albino Rat. A Histological and Immunohistochemical Study. Egyptian Journal of Histology. 2017; 40(1): 37–51.

26. Bhang SH, Cho SW, La WG, Lee TJ, Yang HS, Sun AY, Baek SH, Rhie JW, Kim BS. Angiogenesis in ischemic tissue produced by spheroid grafting of human adipose-derived stromal cells. Biomaterials. 2011 Apr;32(11):2734–47.

27. National Research Council (US) Committee for the Update of the Guide for the Care and Use of Laboratory Animals. Guide for the Care and Use of Laboratory Animals. 8th ed. Washington (DC): National Academies Press (US); 2011.

28. You D, Jang MJ, Kim BH, Song G, Lee C, Suh N, Jeong IG, Ahn TY, Kim CS. Comparative study of autologous stromal vascular fraction and adipose-derived stem cells for erectile function recovery in a rat model of cavernous nerve injury. Stem Cells Transl Med. 2015 Apr;4(4):351–8.

29. Bourin P, Bunnell BA, Casteilla L, Dominici M, Katz AJ, March KL, Redl H, Rubin JP, Yoshimura K, Gimble JM. Stromal cells from the adipose tissue-derived stromal vascular fraction and culture expanded adipose tissue-derived stromal/stem cells: A joint statement of the International Federation for Adipose Therapeutics and Science

(IFATS) and the International Society for Cellular Therapy (ISCT). Cytotherapy. 2013 Jun;15(6):641–8.

30. Kim SG, You D, Kim K, Aum J, Kim YS, Jang MJ, Moon KH, Kang HW. Therapeutic Effect of Human Mesenchymal Stem Cell-Conditioned Medium on Erectile Dysfunction. World J Mens Health 2021 Dec 28. doi: 10.5534/wjmh.210121. Online ahead of print.
31. Jang MJ, You D, Park JY, Kim K, Aum J, Lee C, Song G, Shin HC, Suh N, Kim YM, Kim CS. Hypoxic Preconditioned Mesenchymal Stromal Cell Therapy in a Rat Model of Renal Ischemia-reperfusion Injury: Development of Optimal Protocol to Potentiate Therapeutic Efficacy. Int J Stem Cells. 2018 Nov 30;11(2):157–67.
32. Veuthey T, Hoffmann D, Vaidya VS, Wessling-Resnick M. Impaired renal function and development in Belgrade rats. American Journal of Physiology-Renal Physiology. 2014 Feb 1;306(3):F333–43.
33. Jia Q, Yang R, Liu XF, Ma SF, Wang L. Genistein attenuates renal fibrosis in streptozotocin‐induced diabetic rats. Molecular medicine reports. 2019 Jan 1;19(1):423–31.
34. Melnikov VY, Faubel S, Siegmund B, Lucia MS, Ljubanovic D, Edelstein CL. Neutrophil-independent mechanisms of caspase-1- and IL-18-mediated ischemic acute tubular necrosis in mice. J Clin Invest. 2002 Oct;110(8):1083–91.
35. d'Angelo M, Cimini A, Castelli V. Insights into the Effects of Mesenchymal Stem Cell-Derived Secretome in Parkinson's Disease. Int J Mol Sci. 2020 Jul 23;21(15):5241.
36. Gnecchi M, Melo LG. Bone Marrow-Derived Mesenchymal Stem Cells: Isolation, Expansion, Characterization, Viral Transduction, and Production of Conditioned Medium. Methods Mol Biol. 2009;482:281–94.
37. Sun B, Guo S, Xu F, Wang B, Liu X, Zhang Y, Xu Y. Concentrated HypoxiaPreconditioned Adipose Mesenchymal Stem Cell-Conditioned Medium

Improves Wounds Healing in Full-Thickness Skin Defect Model. Int Sch Res Notices. 2014 Nov 25;2014:652713.

38. Santos JM, Camões SP, Filipe E, Cipriano M, Barcia RN, Filipe M, Teixeira M, Simões S, Gaspar M, Mosqueira D, Nascimento DS, Pinto-do-Ó P, Cruz P, Cruz H, Castro M, Miranda JP. Three-Dimensional Spheroid Cell Culture of Umbilical Cord Tissue-Derived Mesenchymal Stromal Cells Leads to Enhanced Paracrine Induction of Wound Healing. Stem Cell Res Ther. 2015 May 9;6(1):90.

39. Zhou F, Hui Y, Xu Y, Lei H, Yang B, Guan R, Gao Z, Xin Z, Hou J. Effects of AdiposeDerived Stem Cells plus Insulin on Erectile Function in Streptozotocin-Induced Diabetic Rats. Int Urol Nephrol. 2016 May;48(5):657–69.

40. Hwang SJ, Cho TH, Lee B, Kim IS. Bone-Healing Capacity of Conditioned Medium Derived from Three-Dimensionally Cultivated Human Mesenchymal Stem Cells and Electrical Stimulation on Collagen Sponge. J Biomed Mater Res A. 2018 Feb;106(2):311–20.

41. Liu L, Gao J, Yuan Y, Chang Q, Liao Y, Lu F. Hypoxia preconditioned human adipose derived mesenchymal stem cells enhance angiogenic potential via secretion of increased VEGF and bFGF. Cell Biol Int. 2013 Jun;37(6):551–60.

42. Hu X, Yu SP, Fraser JL, Lu Z, Ogle ME, Wang JA, Wei L. Transplantation of hypoxia-preconditioned mesenchymal stem cells improves infarcted heart function via enhanced survival of implanted cells and angiogenesis. J Thorac Cardiovasc Surg. 2008 Apr;135(4):799–808.

43. Hsiao ST, Lokmic Z, Peshavariya H, Abberton KM, Dusting GJ, Lim SY, Dilley RJ. Hypoxic conditioning enhances the angiogenic paracrine activity of human adipose-derived stem cells. Stem Cells Dev. 2013 May 15;22(10):1614–23.

44. Byrne MB, Leslie MT, Gaskins HR, Kenis PJA. Methods to study the tumor microenvironment under controlled oxygen conditions. Trends Biotechnol. 2014 Nov;32(11):556–63.

45. Korff T, Kimmina S, Martiny-Baron G, Augustin HG. Blood vessel maturation in a 3-dimensional spheroidal coculture model: direct contact with smooth muscle cells regulates endothelial cell quiescence and abrogates VEGF responsiveness. FASEB J. 2001 Feb;15(2):447–57.

46. Zhou L, Xu L, Shen J, Song Q, Wu R, Ge Y, Xin H, Zhu J, Wu J, Jia R. Preischemic Administration of Nonexpanded Adipose Stromal Vascular Fraction Attenuates Acute Renal Ischemia/Reperfusion Injury and Fibrosis. Stem Cells Transl Med. 2016 Sep;5(9):1277–88.

47. Wei Q, Wang MH, Dong Z. Differential gender differences in ischemic and nephrotoxic acute renal failure. Am J Nephrol. Sep-Oct 2005;25(5):491–9.

KOREAN ABSTRACT

신장의 허혈-재관류 손상 랫트 모델에서 줄기세포 조정배지와 기질혈관분획 치료의 비교 연구

세포 기반 요법의 다양한 부작용을 피하기 위해 조정배지 요법이 대두되고 있다. 여러 연구에서 다양한 급성 신손상 모델의 치료에 줄기세포 조정배지의 사용에 관심을 가졌다. 그러나 급성 신손상에서 세포 기반 요법과 조정배지 요법의 효과를 비교한 연구는 거의 없다. 따라서, 우리는 허혈-재관류 손상으로 유도된 급성 신손상 랫트 모델에서 자가 기질혈관분획과 3 차원 배양 시스템으로 획득한 지방유래 줄기세포 조정배지가 신기능에 미치는 영향을 비교하였다.

50 마리의 수컷 Sprague-Dawley 랫트를 무작위로 5 개군으로 나누었다: 거짓수술군, 신절제 대조군, 허혈-재관류 손상 대조군, 기질혈관분획군, 지방유래 줄기세포 조정배지군. 기질혈관분획과 지방유래 줄기세포는 각각의 랫트의 고환 주위 지방을 이용하여 분리 및 배양하였다. 지방유래 줄기세포 조정배지는 3 차원 배양 시스템을 사용하여 획득하였다. 허혈-재관류 손상 대조군, 기질혈관분획군 및 지방유래 줄기세포 조정배지군에서 비히클, 기질혈관분획 및 지방유래 줄기세포 조정배지를 각각 신실질에 주입하였다. 허혈-재관류 손상 전 28 일과 손상 후 1, 2, 3, 4, 7, 14 일에 신기능을 평가하였으며, 손상 후 14 일째에 랫트를 희생시킨 후 조직학적 검사를 위해 신장 조직을 채취하였다.

지방유래 줄기세포 조정배지의 신실질 주사는 허혈-재관류 손상 후 1, 2, 3, 4 일째에 허혈-재관류 손상 대조군에 비해 혈청 혈액요소질소 상승 수준을 유의하게 감소시켰다. 혈청 혈액요소질소 수치는 손상 후 1 일과 4 일에 기질혈관분획군보다 지방유래 줄기세포 조정배지군에서 유의하게 낮았다. 지방유래 줄기세포 조정배지의 신실질 주사는 손상 후 1, 2, 3, 4 일째에 허혈-재관류 손상 대조군에 비해 혈청 크레아티닌 상승 수준을 유의하게 감소시켰다. 혈청 크레아티닌 수치는 손상 4 일 후 지방유래 줄기세포 조정배지군이 기질혈관분획군보다 유의하게 낮았다. 지방유래 줄기세포 조정배지의 신실질 주사는 손상 1 일 후 허혈-재관류 손상 대조군에 비해 사구체여과율 감소 수준을 유의하게 감소시켰다. 사구체여과율은 손상 1 일 후 기질혈관분획군보다 지방유래 줄기세포 조정배지군에서 유의하게 더 높았다. 또한 콜라겐 함량은 피질과 수질 모두에서 허혈-재관류 손상 대조군보다 기질혈관분획 및 지방유래 줄기세포 조정배지군에서 유의하게 낮았다. 허혈-재관류 손상 대조군에 비해 기질혈관분획군과 지방유래 줄기세포 조정배지군에서 세포사멸은 피질과 수질 모두에서 유의하게 감소하였고, 세포증식은 유의하게 증가하였다. 글루타티온 환원효소, 글루타티온 퍼옥시다제와 같은 항산화 표지자의 발현은 피질과 수질 모두에서 허혈-재관류 손상 대조군보다 기질혈관분획군과 지방유래 줄기세포 조정배지군에서 더 높았다.

지방유래 줄기세포 조정배지의 신실질 주입은 향상된 항섬유화, 항세포사멸 및 항산화 효과를 통해 신장 허혈-재관류 손상으로부터 신기능을 효과적으로 보호한다. 지방유래 줄기세포 조정배지는 신장 허혈-재관류 손상 후 초기에 혈청 혈액요소질소, 혈청 크레아티닌, 사구체여과율 측면에서 기질혈관분획보다 우월했으나, 손상 7 일 이후에 그 차이가 사라졌다.